Supporting Information

Inactivation of Flavoenzyme-Encoding Gene *flsO1* in Fluostatin Biosynthesis Leads to Diversified Angucyclinone Derivatives

Chunfang Yang,[†,‡,§,⊥] Chunshuai Huang,[†,Δ,⊥] Chunyan Fang,[†,Δ] Liping Zhang,[†,‡,§] Siqiang Chen,[†,Δ] Qingbo Zhang,[†,‡,§] Changsheng Zhang,[*,†,‡,§,Δ] and Wenjun Zhang[*,†,‡,§,Δ]

[†]*Key Laboratory of Tropical Marine Bio-resources and Ecology, Guangdong Key Laboratory of Marine Materia Medica, Innovation Academy of South China Sea Ecology and Environmental Engineering, South China Sea Institute of Oceanology, Chinese Academy of Sciences, Guangzhou 510301, China*

[‡]*Sanya Institute of Oceanology, SCSIO, Yazhou Scientific Bay, Sanya 572000, China*

[§]*Southern Marine Science and Engineering Guangdong Laboratory (Guangzhou), 1119 Haibin Road, Nansha District, Guangzhou 511458, China*

[Δ]*University of Chinese Academy of Sciences, Beijing 100049, China*

[⊥]These authors contributed equally to this work.

[*]Corresponding author: czhang@scsio.ac.cn or wzhang@scsio.ac.cn

Content

Table S1. Strains and plasmids used and constructed in this study S3
Table S2. Primers used in this study..... S4
Table S3. ^{1}H (700 MHz) and ^{13}C{^{1}H} NMR (176 MHz) Data for **10** and **16** in DMSO-d_6..... S5
Table S4. Crystal data and structure refinement for gephyromycin D (**11**) and a thermal ellipsoid plot (The ellipsoids of non-hydrogen atoms are shown at 50% probability levels)..... S7
Table S5. Crystal data and structure refinement for fluostarene A (**14**) and a thermal ellipsoid plot (The ellipsoids of non-hydrogen atoms are shown at 50% probability levels)..... S8
Table S6. Crystal data and structure refinement for fluostarene B (**15**) and a thermal ellipsoid plot (The ellipsoids of non-hydrogen atoms are shown at 50% probability levels)..... S9
Table S7. Antibacterial activities of **14-16**..... S10
Figure S1. Insertional mutagenesis of *flsO1* in *M. rosaria* SCSIO N160 ..... S11
Figure S2. The UV, HPLC and MS of known compounds **6**, **9** and **13** S12
Figure S3. Spectroscopic data for 5-hydroxy-dehydrorabelomycin (**10**)..... S13
Figure S4. Spectroscopic data for gephyromycin D (**11**)..... S20
Figure S5. Spectroscopic data for 6-hydroxyfridamycin E (**12**) S27
Figure S6. Spectroscopic data for PK1 (**16**)..... S33
Figure S7. Spectroscopic data for fluostarene A (**14**)..... S38
Figure S8. Spectroscopic data for fluostarene B (**15**)..... S44
Figure S9. The HPLC profiles for *S. coelicolor* M1154-3 and *S. coelicolor* M1154-4 with *flsO1* and *alpK trans* complement to Δ*flsO1*i (*S. coelicolor* M1154-2) respectively..... S51
Figure S10. The proposed biosynthetic pathway of compounds **6** and **10**−**12**..... S52
Supplementary References S53

Table S1. Strains and plasmids used and constructed in this study

Strains/Plasmids	Characteristic(s)	Sources Reverence
E.coli		
DH5α	Host strain for cloning	Invitrogen
BW25113/ pIJ790	Host strain for PCR targeting	[1]
ET12567	Donor strain for conjugation	[2]
Streptomyces		
S. coelicolor M1154	Host strain for heterologous expression	[3]
S. coelicolor M1154-1	*S. coelicolor* M1154 contain plasmid pCSG5033	This study
S. coelicolor M1154-2	*S. coelicolor* M1154 contain plasmid pCSG5042 (Δ*flsO1*i)	This study
S. coelicolor M1154-3	With pCSG5043 complement *S.* M1154-2	This study
S. coelicolor M1154-4	With pCSG5044 complement *S.* M1154-2	This study
S. coelicolor M1154-5	Heterologous expression host strain contain plasmid pSET152	This study
M. rosaria		
SCSIO N160	Wild type, fluostatin (**1**–**5**) producer	[4]
FLS08	*flsO1* inserted mutation in SCSIO N160	This study
Streptomyces ambofaciens* Δ*alp1U	template for gene amplification of *alpK*	[5]
Plasmids		
pIJ773	Apr^r, source of *aac(3)IV*	[6]
pIJ778	Spe^r, source of *aadA*	[6]
BT340	Amp^r, Chl^r, temperature sensitive FLP recombination plasmid	[7]
pUZ8002	Km^r, including *tra* for conjugation	[6]
pSET152	*OriT*RK2 (origin of conjugal transfer) *attP* (φC31 attachment site)	[8]
pPWW50A	Apr^r, template for amplifying *ermE**p promoter	[9]
pPM927	Spe^r / $Strep^r$ and Thi^r, *attP* (φC31 attachment site), *tipA* promoter	[10]
pCSG5001	Strain SCSIO N160 genomic library cosmid	This study
pCSG5013	pCSG5001 derivative where *flsO1* was disrupted by *aac(3)IV*	This study
pCSG5033	pCSG5003 derivative where Km^r gene was replaced by sequence from pSET152AB with *Bam*HI and *Eco*RI digesting	This study
pCSG5042	pCSG5033 derivative where *flsO1* was in-frame deleted via BT340 mediated tailoring	This study
pCSG5043	*erm-flsO1* was inserted to pPM927 vector	This study
pCSG5044	*erm-alpK* was inserted to pPM927 vector	This study

Table S2. Primers used in this study

Primers	Gene	Sequences
For gene disruption		
flsO1DF	*flsO1*	5'-GAGCCCATGCAGCAGTCGCGCGCCCTGGGTTTCTCGGCCattccggggatccgtcgacc-3'
flsO1DR		5'-GCCGTGGAACGGGTCGTCCGGGTCGGCGGTGTGCGGCGTtgtaggctggagctgcttc-3'
For PCR confirmation of mutants' genotype		
flsO1DTF	*flsO1*	5'-ATCATCGTAGGAGCCGGACC-3'
flsO1DTR		5'-GCCGAACCAGCGCGACAGGG-3'
For constructing complement vectors of *flsO1* and *alpK*		
927-*erm*F	*erm-flsO1*	5'-AAGCCGGCGACCCAGGGATCCCAGGCGGTACCAGCCCGACC-3'
*erm-flsO1*R		5'-TCCGCATCGATTGTGTTCATGGTTCGCCCGCTCTCCT-3'
flsO1-F		5'-GAGAGGAGAGCGGGCGAACCATGAACACAATCGATGCGGA-3'
flsO1-927R		5'-GCGAGCTCGAATTGGGGATCCTCAGCGGGACGGGCCGAAC-3'
927-*erm*F	*erm-alpK*	5'-AAGCCGGCGACCCAGGGATCCCAGGCGGTACCAGCCCGACC-3'
*erm-alpK*R		5'-GTCCGAATCGTAGAATTCCATGGTTCGCCCGCTCTCCT-3'
alpK-F		5'-GAGAGGAGAGCGGGCGAACCATGGAATTCTACGATTCGGA-3'
alpK-927R		5'-GCGAGCTCGAATTGGGGATCCTCAGGCGGTGGGGCCGAAC-3'

Table S3. ^{1}H (700 MHz) and ^{13}C{^{1}H} NMR (176 MHz) Data for **10** and **16** in DMSO-d_6

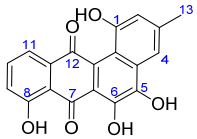

10

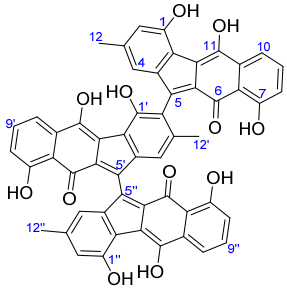

16

No.	10		No.	16	
	δ_C type	δ_H multi (J in Hz)		δ_C type	δ_H multi (J in Hz)
1	155.3 C		1	148.8 C	
2	118.1 CH	6.80 s	2	115.6 CH	5.85s
3	139.2 C		3	137.7 C	
4	113.6 CH	7.51 s	4	117.7 CH	6.17 s
4a	130.2 C		4a	146.1 C	
5	154.4 C		5	149.2 C	
6	158.2 C		5a	N	
6a	119.3 C		6	185.2 C	
7	193.1 C		6a	N	
7a	115.3 C		7	162.9 C	
8	160.8 C		8	114.3 C	7.19 d (7.52)
9	122.7 CH	7.26 d (8.3)	9	135.7 C	7.40 dd (7.51, 7.71)
10	138.0 CH	7.76 dd (7.4, 8.3)	10	116.6 C	6.90 d (7.71)
11	119.7 CH	7.66 d (7.4)	10a	134.3 C	
11a	136.8 C		11	162.9 C	
12	181.0 C		11a	118.1 C	
12a	144.7 C		11b	120.4 C	
12b	119.8 C		12	21.3 CH_3	1.86 s
13	21.4 CH_3	2.37 s	7-OH		12.97 s
6-OH		12.64 brs	1'	150.8 C	
8-OH		11.63 s	2'	123.3 C	
			3'	134.2 C	
			4'	115.8 CH	6.66 s
			4a'	141.2 C	
			5'	141.2 C	
			5a'	N	
			6'	186.3 C	
			6a'	N	

	7'	162.9 C	
	8'	114.7 C	7.45 d (7.54)
	9'	136.4 C	7.51 dd (8.12, 7.54)
	10'	116.0 C	6.87 d (8.12)
	11'	162.9 C	
	11a'	119.5 C	
	11b'	N	
	12'	20.1 CH_3	1.94 s
	7'-OH		13.03 s
	1"	148.8 C	
	2"	115.7 CH	5.82 s
	3"	137.9 C	
	4"	118.1 CH	6.14 s
	4a"	146.7 C	
	5"	149.7 C	
	6"	185.7 C	
	6a"		
	7"	162.9 C	
	8"	114.8 C	7.16 d (7.84)
	9"	135.8 C	7.40 dd (7.84, 7.67)
	10"	117.2 C	6.90 d (7.67)
	10a"	134.5 C	
	11"	162.9 C	
	11a"	119.7 C	
	11b"	120.6 C	
	12"	21.4 CH_3	1.86 s
	7"-OH		12.97 s

Table S4. Crystal data and structure refinement for gephyromycin D (**11**) and a thermal ellipsoid plot (The ellipsoids of non-hydrogen atoms are shown at 50% probability levels).

Identification code	gephyromycin D
Empirical formula	$C_{19}H_{16}O_8$ (without solvent)
Formula weight	372.32
Temperature/K	99.9(7)
Crystal system	orthorhombic
Space group	$P2_12_12_1$
a/Å	7.04280(10)
b/Å	16.1794(2)
c/Å	28.9977(3)
α/°	90
β/°	90
γ/°	90
Volume/Å^3	3304.24(7)
Z	8
ρ_{calc}g/cm^3	1.526
μ/mm^{-1}	1.028
F(000)	1584.0
Crystal size/mm^3	0.05 × 0.03 × 0.03
Radiation	Cu Kα (λ = 1.54184)
2Θ range for data collection/°	8.188 to 148.114
Index ranges	$-8 \leq h \leq 8$, $-19 \leq k \leq 14$, $-35 \leq l \leq 32$
Reflections collected	12148
Independent reflections	6019 [R_{int} = 0.0389, R_{sigma} = 0.0544]
Data/restraints/parameters	6019/0/519
Goodness-of-fit on F^2	1.049
Final R indexes [I>=2σ (I)]	R_1 = 0.0423, wR_2 = 0.1050
Final R indexes [all data]	R_1 = 0.0512, wR_2 = 0.1089
Largest diff. peak/hole / e Å^{-3}	0.39/-0.25
Flack parameter	-0.14(13)

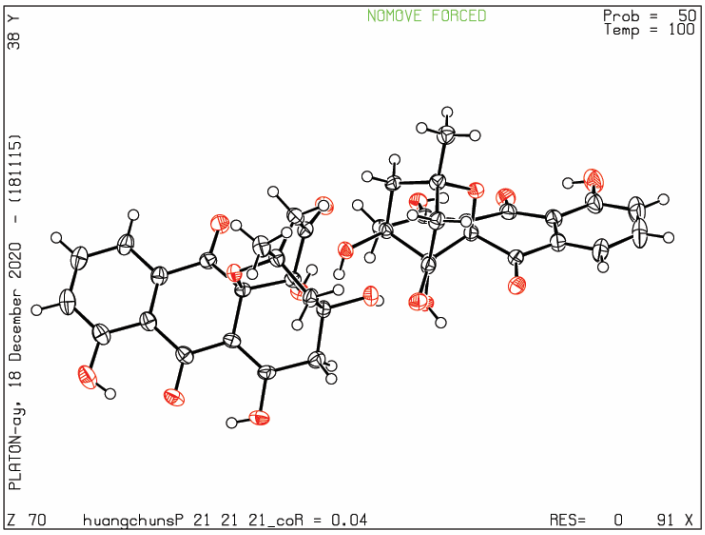

Table S5. Crystal data and structure refinement for fluostarene A (**14**) and a thermal ellipsoid plot (The ellipsoids of non-hydrogen atoms are shown at 50% probability levels).

Identification code	fluostarene A
Empirical formula	$C_{26}H_{18}O_7$ (without solvent)
Formula weight	442.40
Temperature/K	105(7)
Crystal system	triclinic
Space group	P-1
a/Å	7.3082(5)
b/Å	11.9117(6)
c/Å	12.1863(7)
α/°	70.129(5)
β/°	85.638(5)
γ/°	88.680(5)
Volume/Å^3	994.80(11)
Z	2
ρ_{calc}g/cm^3	1.477
μ/mm^{-1}	0.900
F(000)	460.0
Crystal size/mm^3	0.1 × 0.1 × 0.1
Radiation	Cu Kα (λ = 1.54184)
2Θ range for data collection/°	7.734 to 148.02
Index ranges	$-5 \leq h \leq 8$, $-14 \leq k \leq 14$, $-15 \leq l \leq 15$
Reflections collected	9061
Independent reflections	3845 [R_{int} = 0.0455, R_{sigma} = 0.0500]
Data/restraints/parameters	3845/0/312
Goodness-of-fit on F^2	1.072
Final R indexes [I>=2σ (I)]	R_1 = 0.0557, wR_2 = 0.1530
Final R indexes [all data]	R_1 = 0.0747, wR_2 = 0.1629
Largest diff. peak/hole / e Å^{-3}	0.41/-0.28

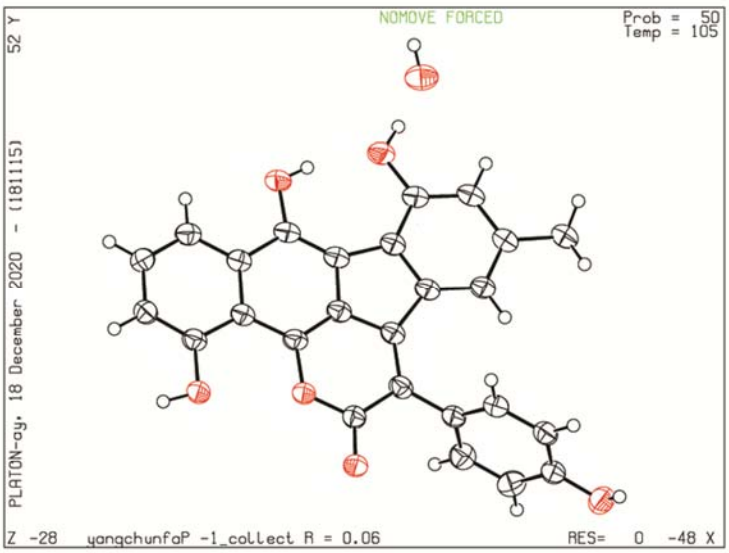

Table S6. Crystal data and structure refinement for fluostarene B (**15**) and a thermal ellipsoid plot (The ellipsoids of non-hydrogen atoms are shown at 50% probability levels).

Identification code	fluostarene B
Empirical formula	$C_{29}H_{21}NO_6$ (without solvent)
Formula weight	479.47
Temperature/K	99.9(9)
Crystal system	monoclinic
Space group	P21/c
a/Å	16.3314(6)
b/Å	10.4242(3)
c/Å	13.4202(5)
α/°	90
β/°	112.431(4)
γ/°	90
Volume/Å^3	2111.82(14)
Z	4
ρ_{calc}g/cm^3	1.508
μ/mm^{-1}	0.875
F(000)	1000.0
Crystal size/mm^3	0.1 × 0.1 × 0.05
Radiation	Cu Kα (λ = 1.54184)
2Θ range for data collection/°	10.312 to 147.782
Index ranges	$-19 \leq h \leq 20$, $-9 \leq k \leq 12$, $-16 \leq l \leq 16$
Reflections collected	11504
Independent reflections	4168 [R_{int} = 0.0403, R_{sigma} = 0.0481]
Data/restraints/parameters	4168/0/334
Goodness-of-fit on F^2	1.042
Final R indexes [I>=2σ (I)]	R_1 = 0.0429, wR_2 = 0.1126
Final R indexes [all data]	R_1 = 0.0549, wR_2 = 0.1202
Largest diff. peak/hole / e Å^{-3}	0.23/-0.23

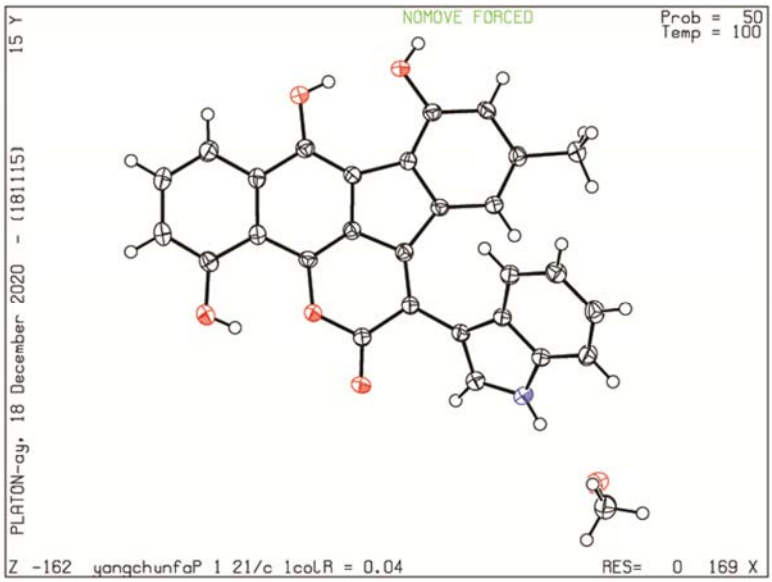

Table S7. Antibacterial activities of **14-16**.

Compounds	MIC (μg·mL^{-1})		
	S.aureus ATCC 29213	*V.alginolyticus* 13214	MRSA shhs-A1
14	>64	>64	>64
15	>64	>64	>64
16	32	64	16
vancomycin[a]	1	64	1

[a]Vancomycin was used as positive control of antibacterial activity. Except **16** show weak activities against *Staphylococcus aureus* ATCC 29213, methicillin-resistant *S. aureus* (MRSA) shhs-A1, *Vibrio alginolyticus* 13214 with MIC of 32, 16 and 64 μg/mL respectively. None of **11**−**12** or **14**−**15** exhibited antibacterial activities towards four pathogenic bacteria, including S*taphylococcus aureus* ATCC 29213, methicillin-resistant *S. aureus* (MRSA) shhs-A1, *Vibrio alginolyticus* 13214 and *Acinetobacter baumannii* ATCC19606.

Figure S1. Insertional mutagenesis of *flsO1* in *M. rosaria* SCSIO N160.

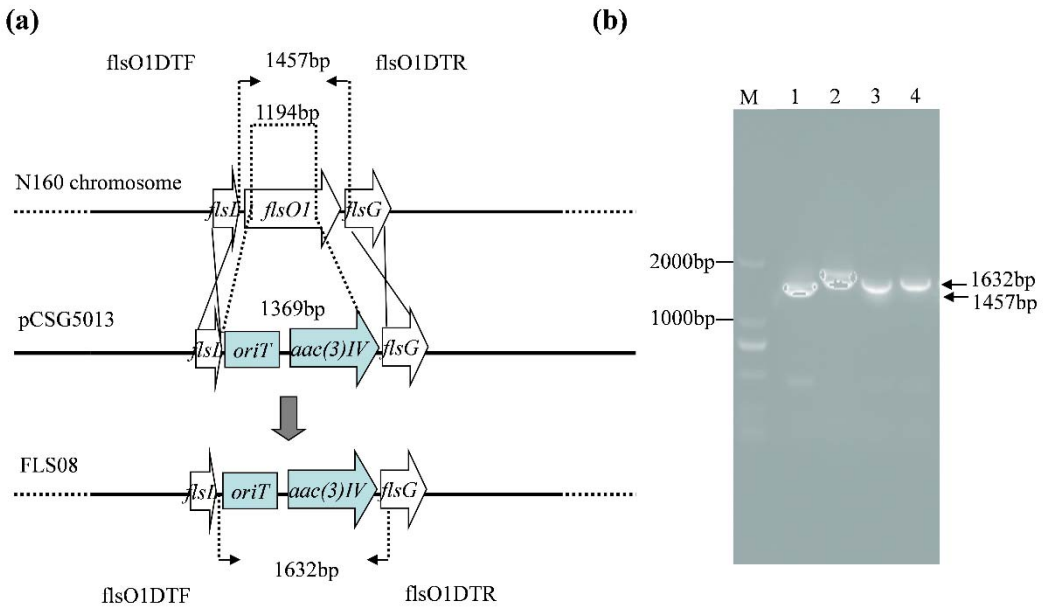

Construction *flsO1* disruption mutant FLS08. (a) Description of *flsO1* disruption. pCSG5013 was constructed by replacing a 1194 bp internal fragment of *flsO1* with a 1369 bp DNA fragment containing *oriT* and *aac3(IV)* in pCSG5001. The location of the diagnostic PCR primers were indicated. Sizes of PCR products were also indicated: 1457 bp for the wild type strain SCSIO N160 and 1632 bp for the mutant FLS08 (b) Gel electrophoresis of PCR products. DNA templates were from: pCSG5001 (negative control, lane 1), pCSG5013 (positive control, lane 2), FLS08 (lane 3 and lane 4) and DNA marker D2000 (GenStar, laneM).

Figure S2. The UV, HPLC and MS of known compounds **6, 9** and **13**.

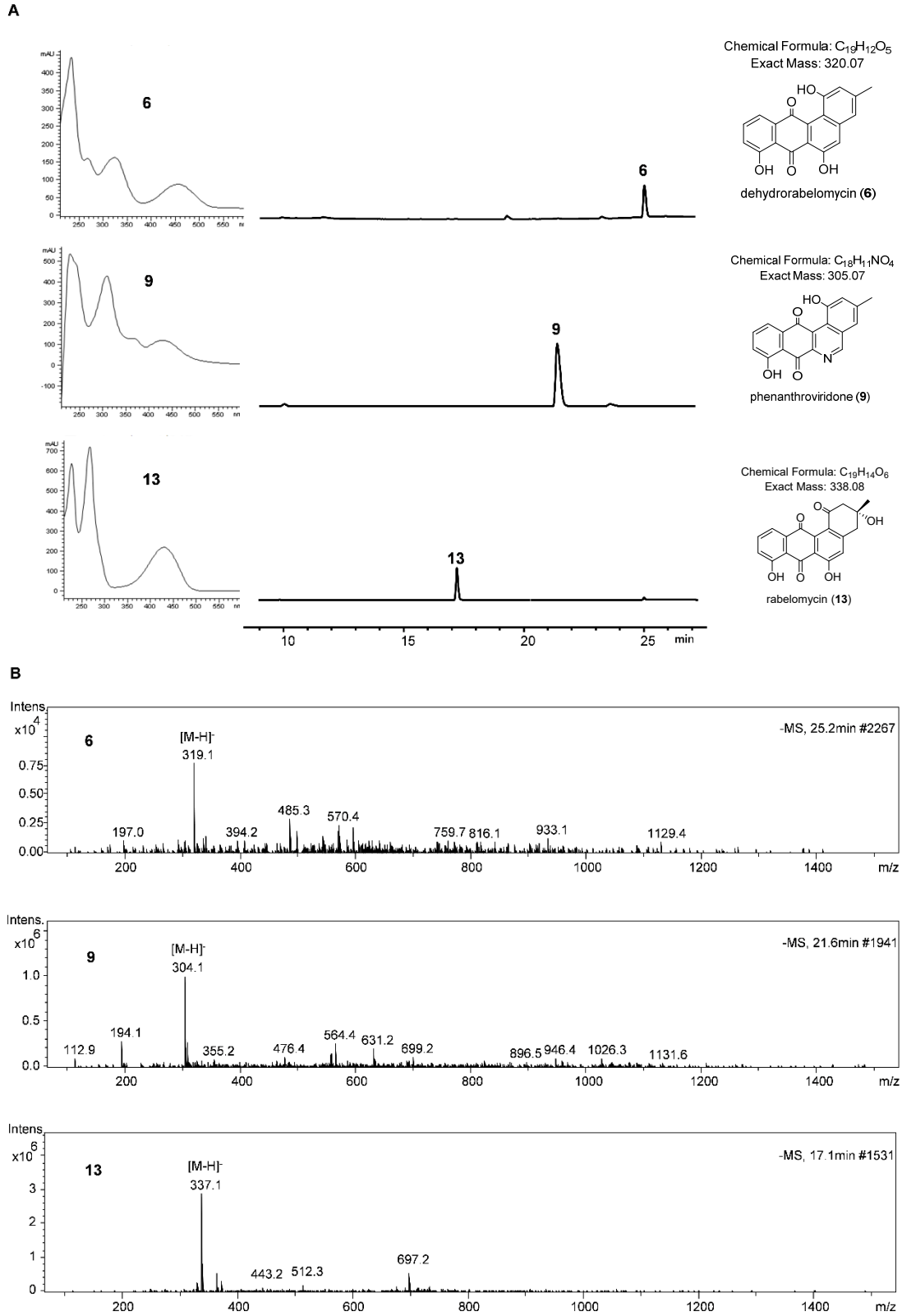

A: The HPLC and UV spectrum of **6**, **9** and **13**. B: The mass of **6**, **9** and **13**.

Figure S3. Spectroscopic data for 5-hydroxy-dehydrorabelomycin (**10**).
(**A**) HRESIMS (**a**), IR (**b**), and UV (**c**) spectra of 5-hydroxy-dehydrorabelomycin (**10**).
(a) HRESIMS

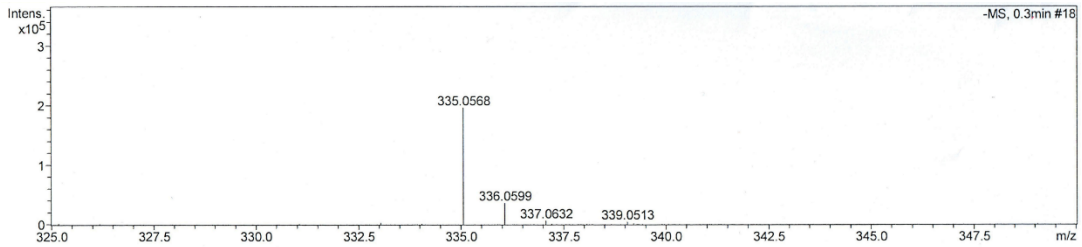

b) IR.

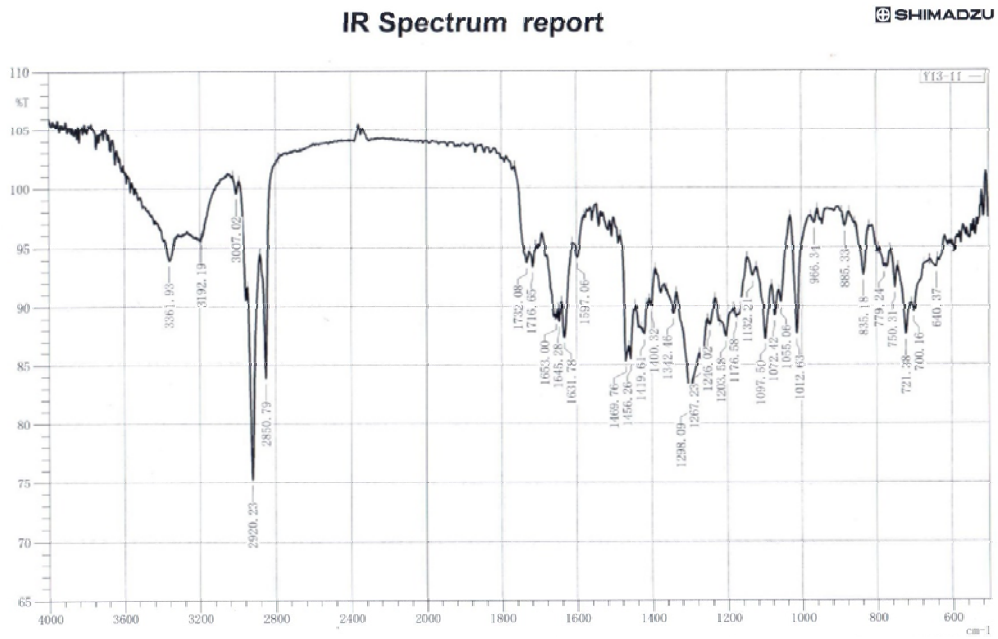

c) UV.

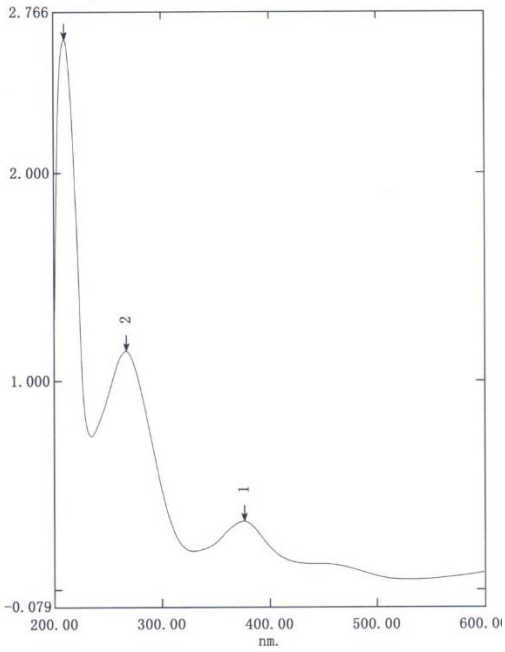

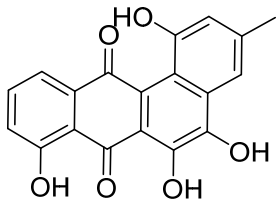

10

Figure S3. Spectroscopic data for 5-hydroxy-dehydrorabelomycin (**10**).
(**B**) The ^{1}H NMR (700 MHz) spectrum of 5-hydroxy-dehydrorabelomycin (**10**) in DMSO-d_6.

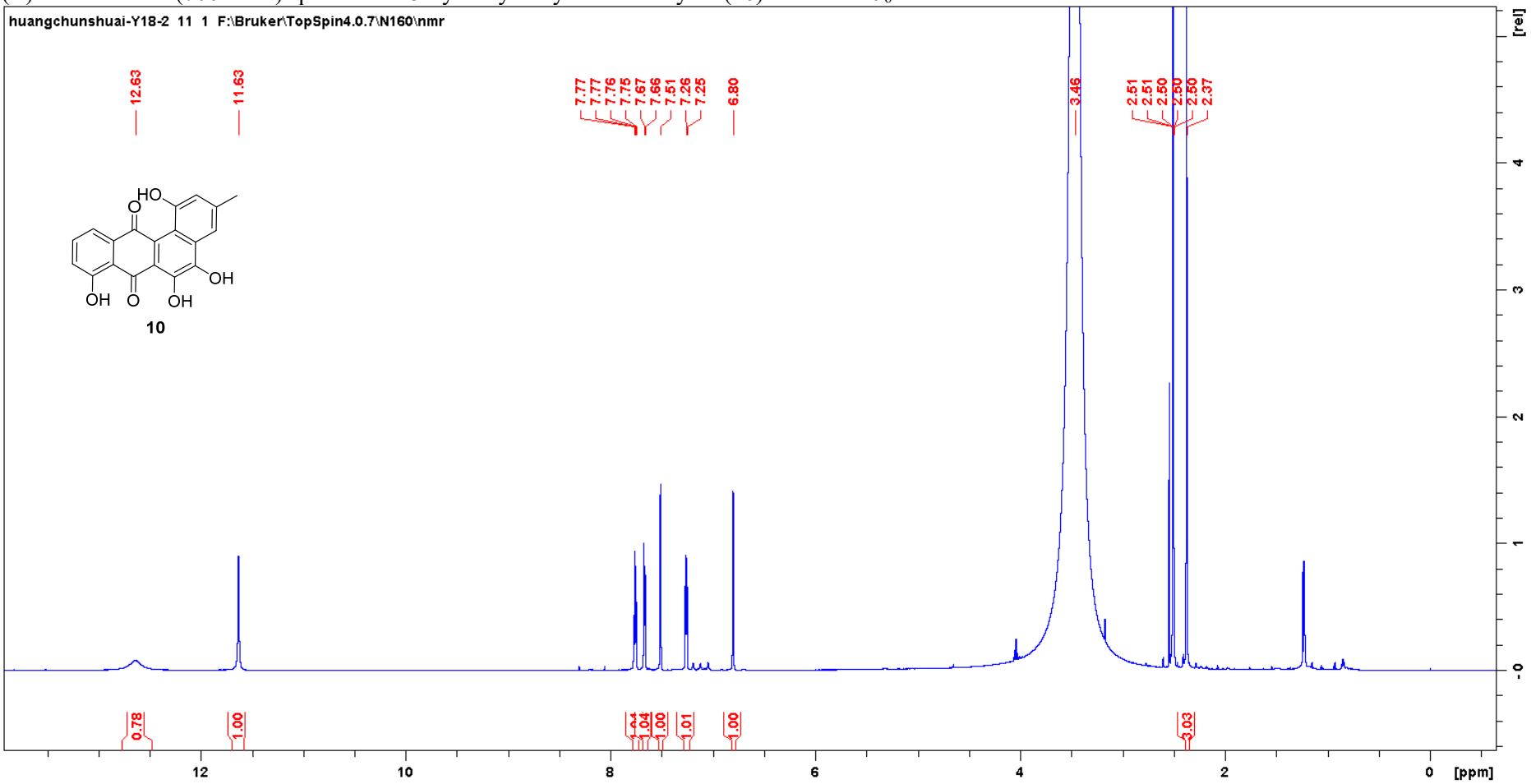

Figure S3. Spectroscopic data for 5-hydroxy-dehydrorabelomycin (**10**). (continued).
(**C**) The $^{13}C\{^{1}H\}$ (176 MHz) spectrum of 5-hydroxy-dehydrorabelomycin (**10**) in DMSO-d_6.

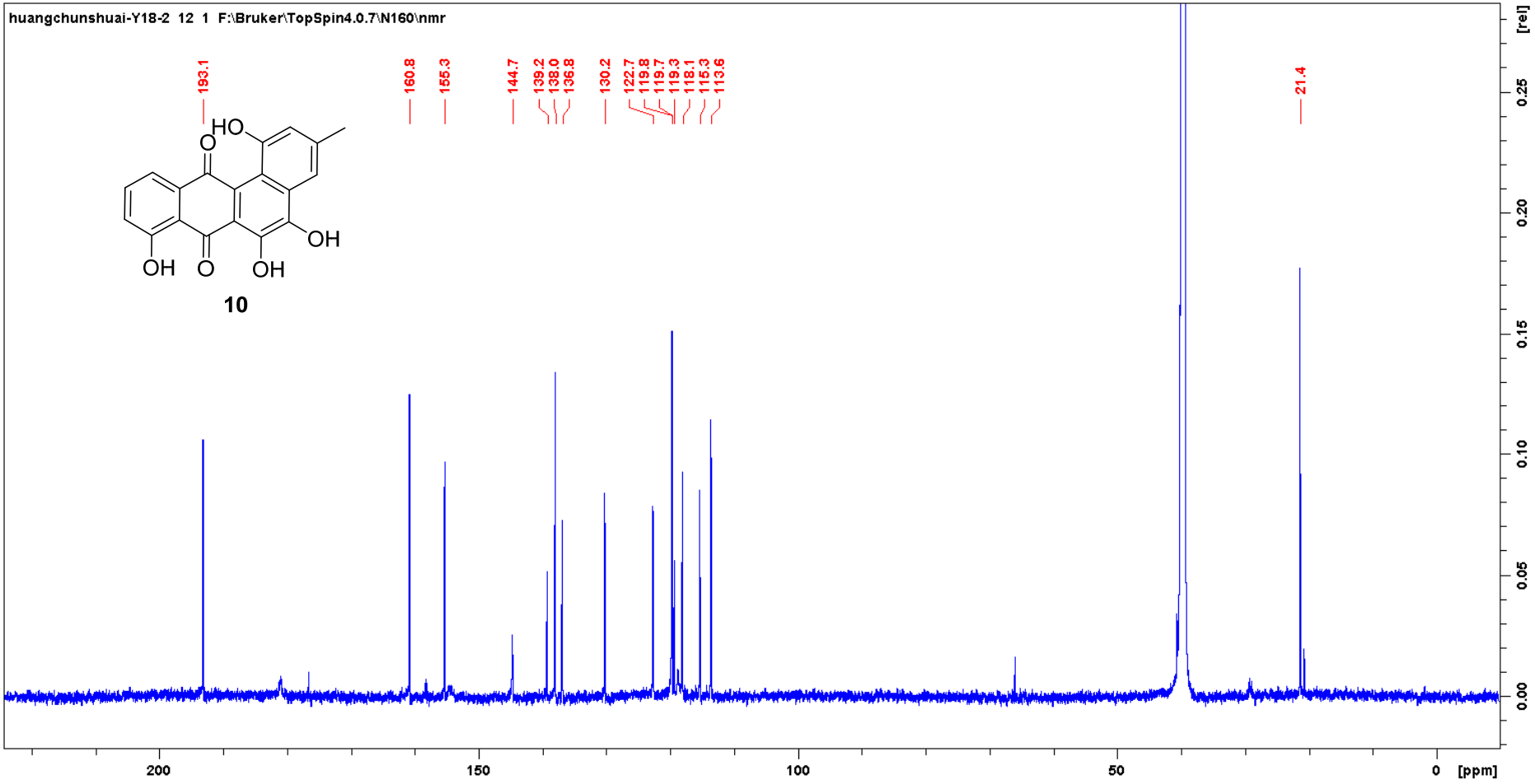

Figure S3. Spectroscopic data for 5-hydroxy-dehydrorabelomycin (**10**). (continued).
(**D**) The DEPT 135 spectrum of 5-hydroxy-dehydrorabelomycin (**10**) in DMSO-d_6.

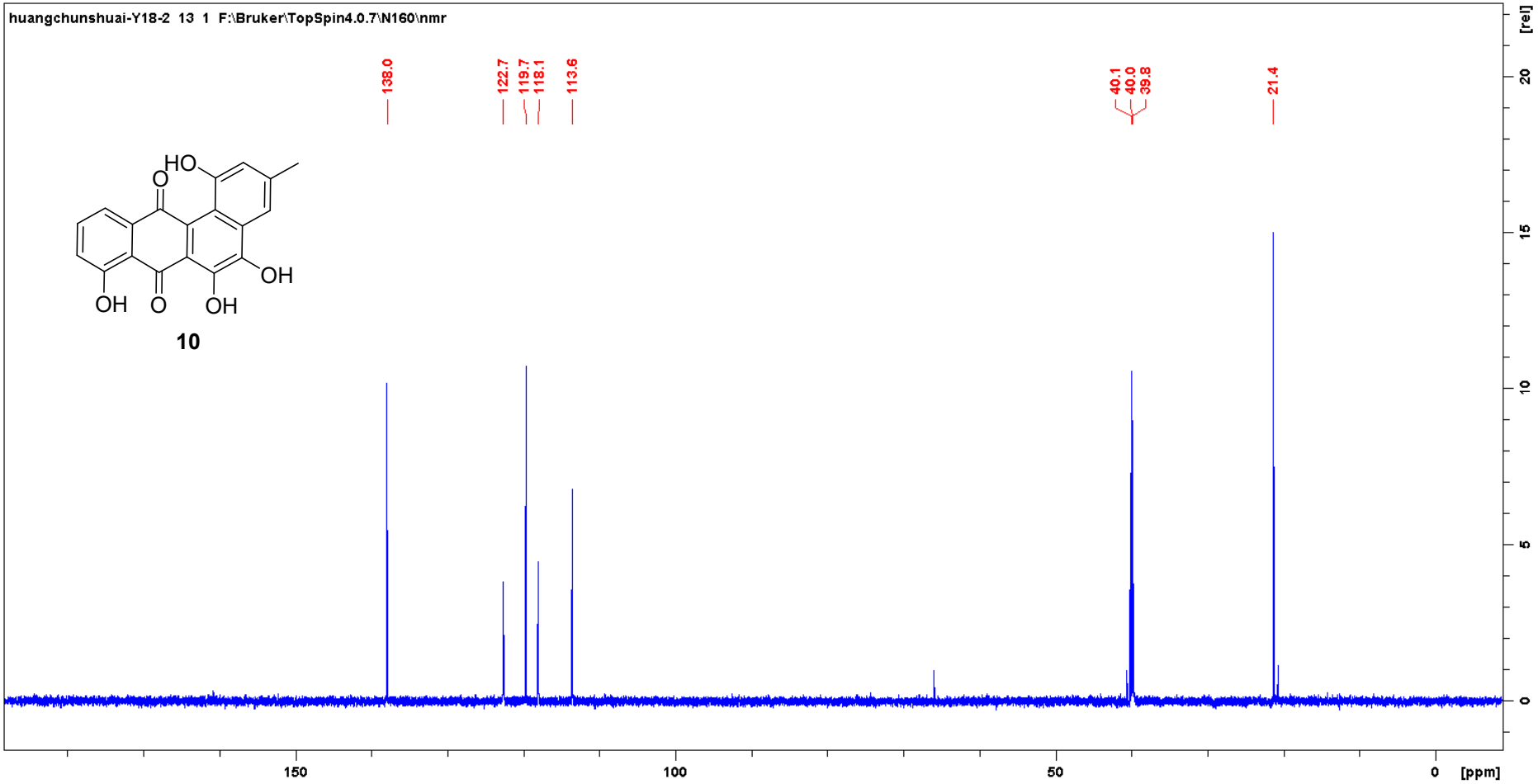

Figure S3. Spectroscopic data for 5-hydroxy-dehydrorabelomycin (**10**). (continued).
(**E**) The HSQC spectrum of 5-hydroxy-dehydrorabelomycin (**10**) in DMSO-d_6.

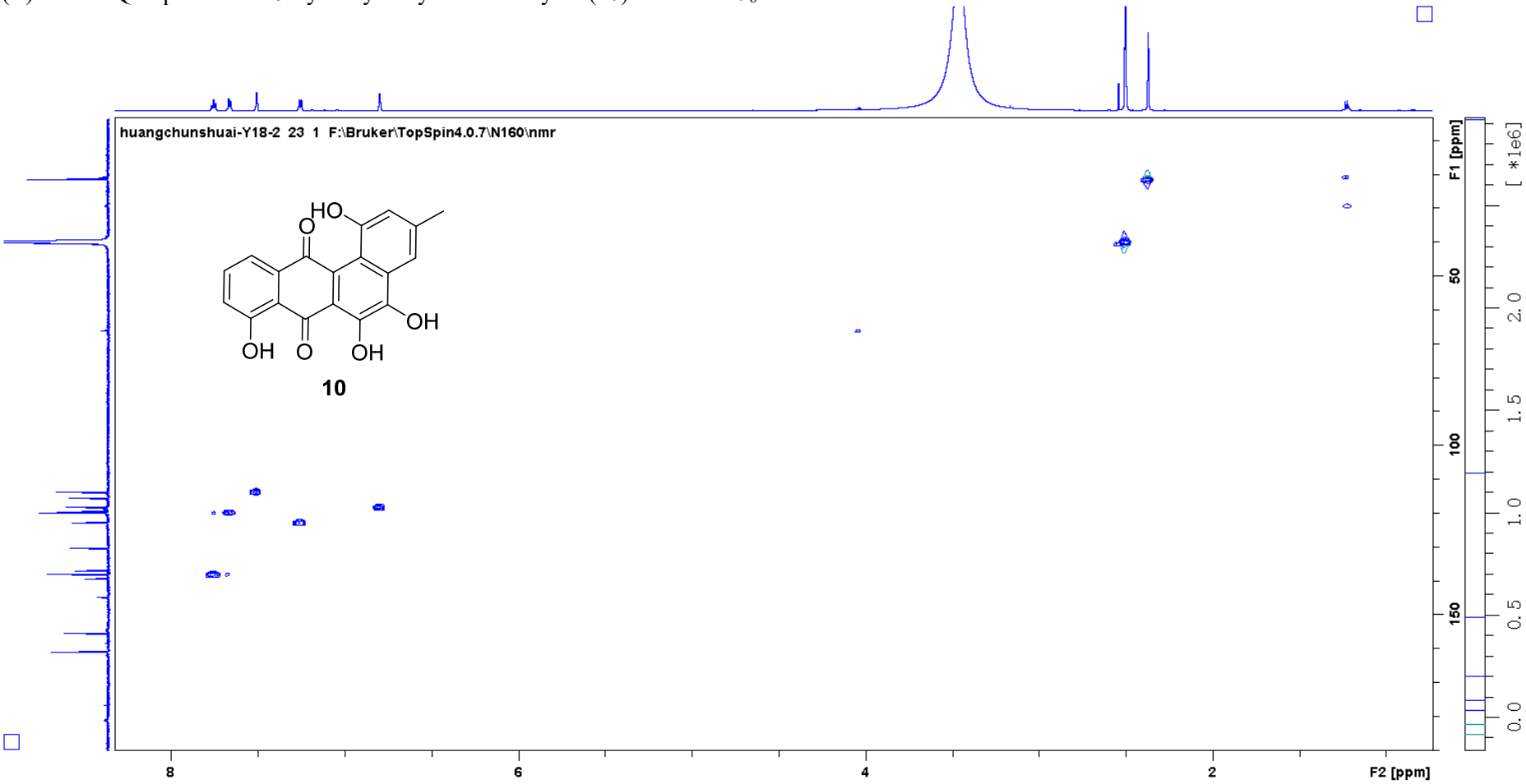

Figure S3. Spectroscopic data for 5-hydroxy-dehydrorabelomycin (**10**). (continued).
(**F**) The COSY spectrum of 5-hydroxy-dehydrorabelomycin (**10**) in DMSO-d_6.

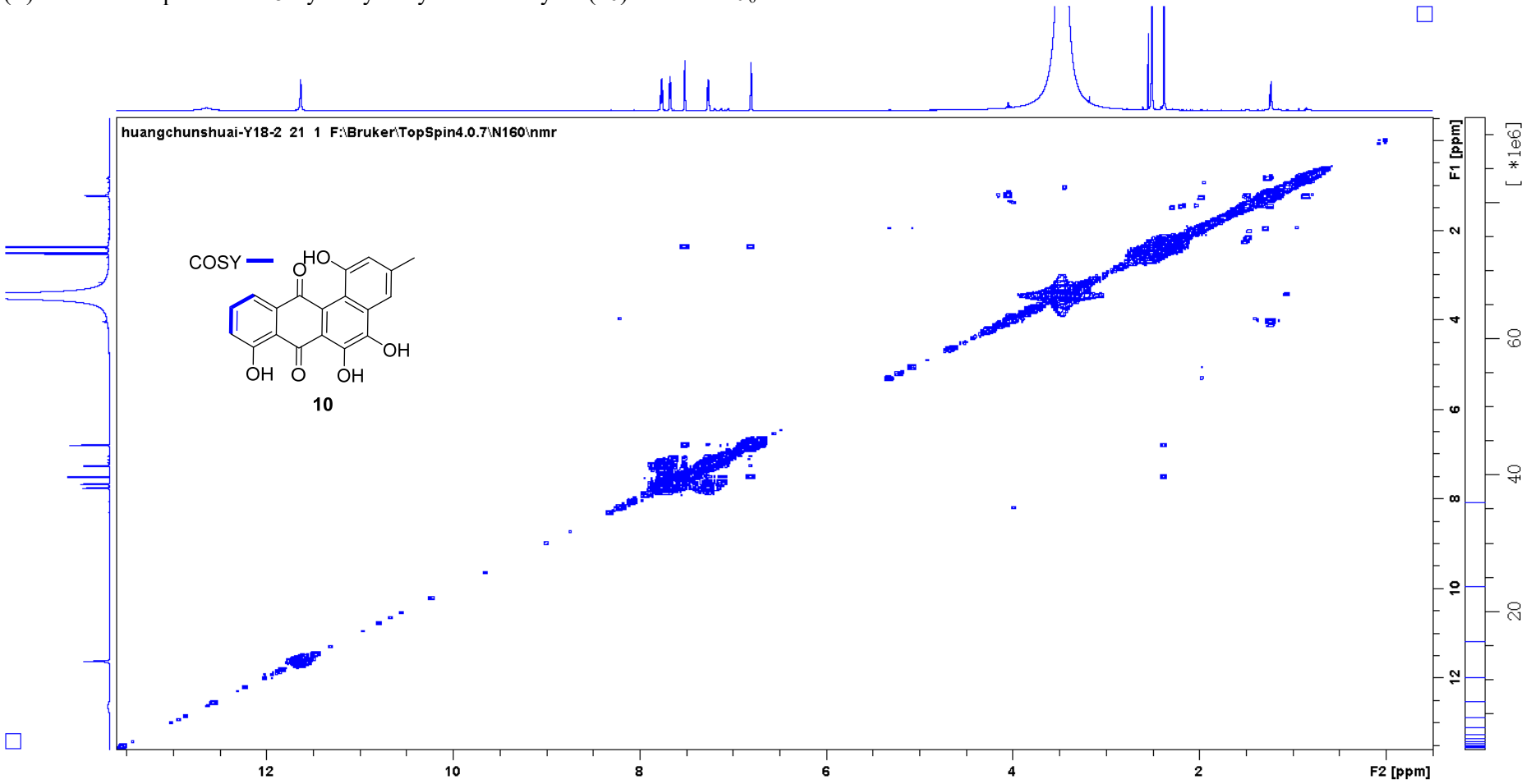

Figure S3. Spectroscopic data for 5-hydroxy-dehydrorabelomycin (**10**). (continued).
(**G**) The HMBC spectrum of 5-hydroxy-dehydrorabelomycin (**10**) in DMSO-d_6.

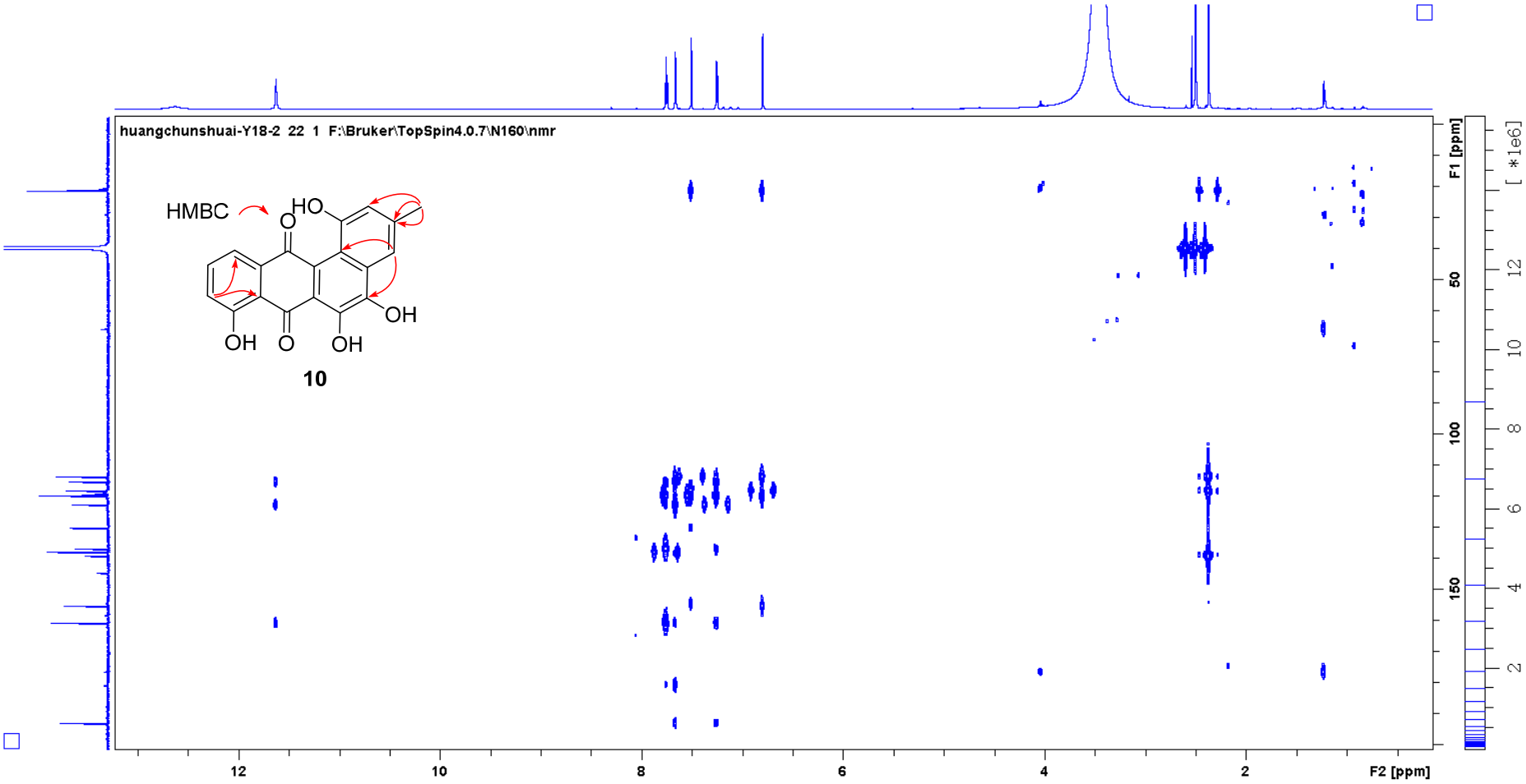

Figure S4. Spectroscopic data for gephyromycin D (**11**).
(**A**) HRESIMS (**a**), IR (**b**), and UV (**c**) spectra of gephyromycin D (**11**).
(a) HRESIMS

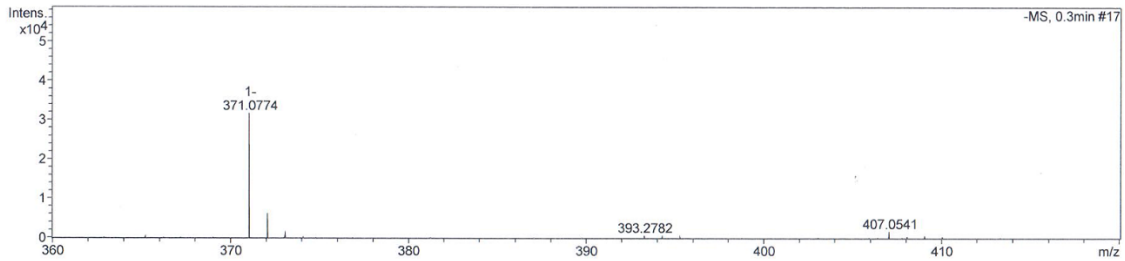

(b) IR.

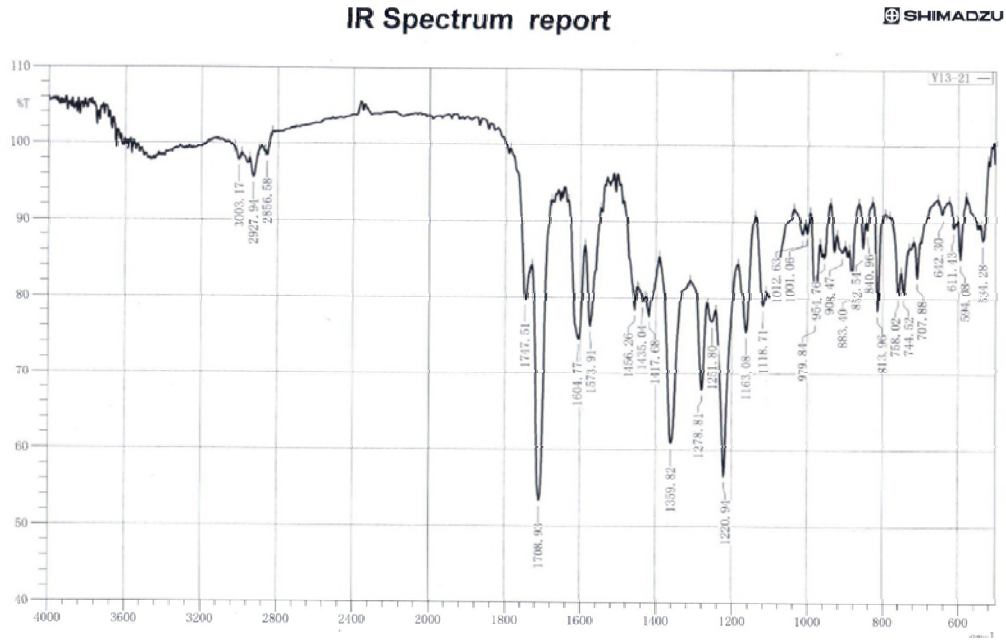

(c) UV.

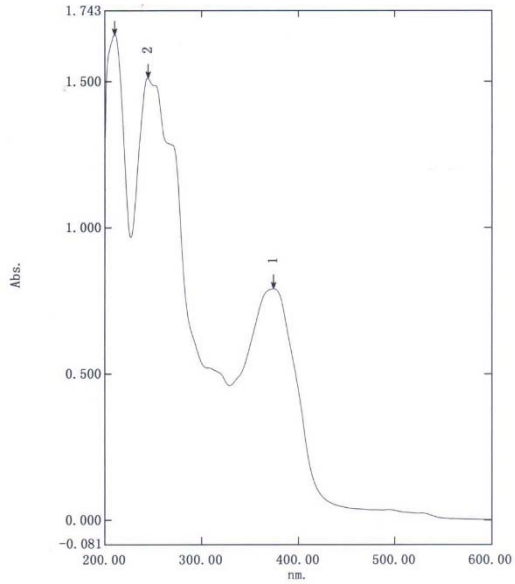

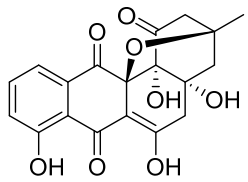

Figure S4. Spectroscopic data for gephyromycin D (**11**). (continued).
(**B**) The ^{1}H NMR spectrum (500 MHz) of gephyromycin D (**11**) in DMSO-d_6.

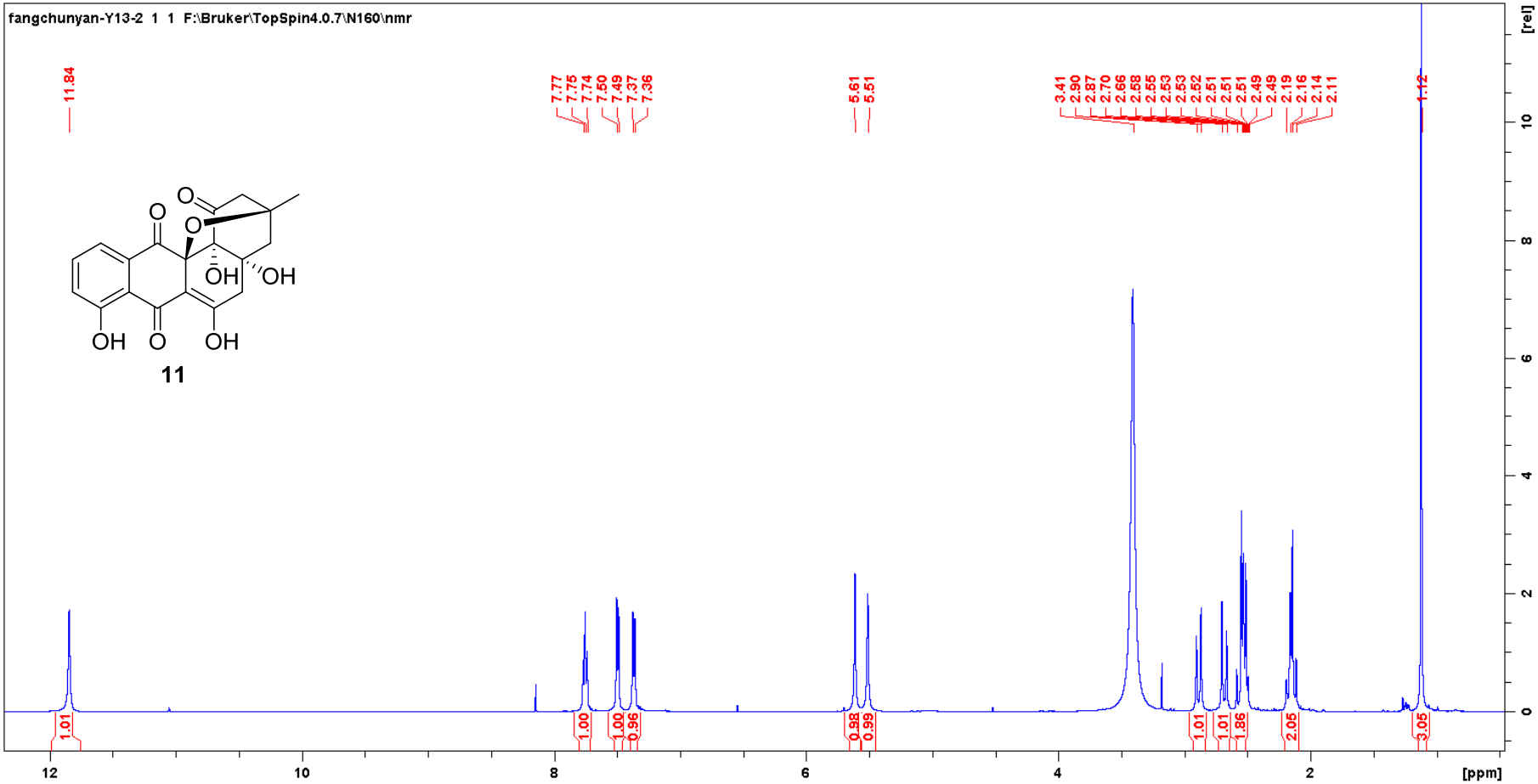

Figure S4. Spectroscopic data for gephyromycin D (**11**). (continued).
(**C**) The $^{13}C\{^{1}H\}$ and DEPT 135 NMR (125 MHz) spectrum of gephyromycin D (**11**) in DMSO-d_6.

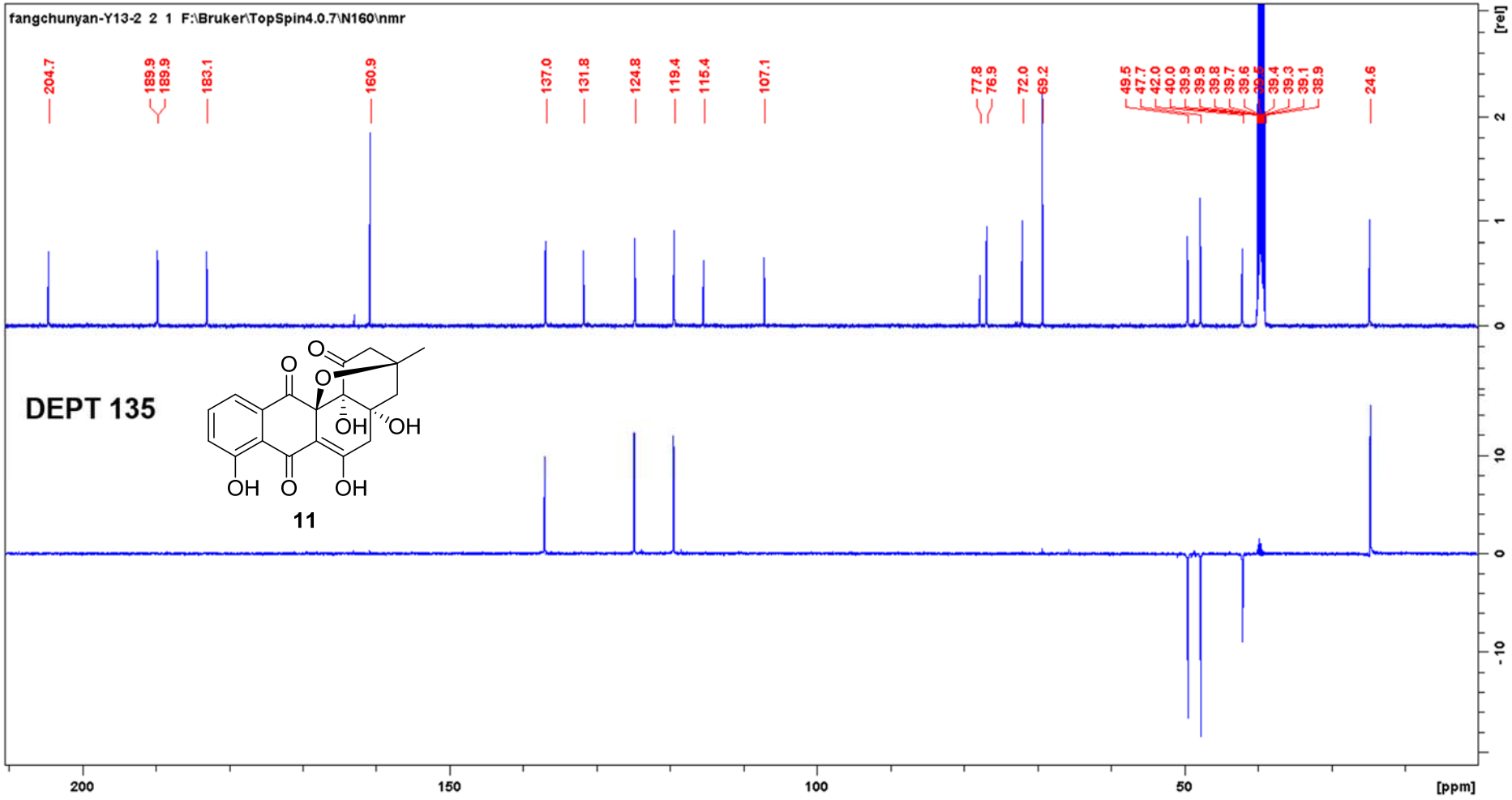

Figure S4. Spectroscopic data for gephyromycin D (**11**). (continued).
(**D**) The HSQC spectrum of gephyromycin D (**11**) in DMSO-d_6.

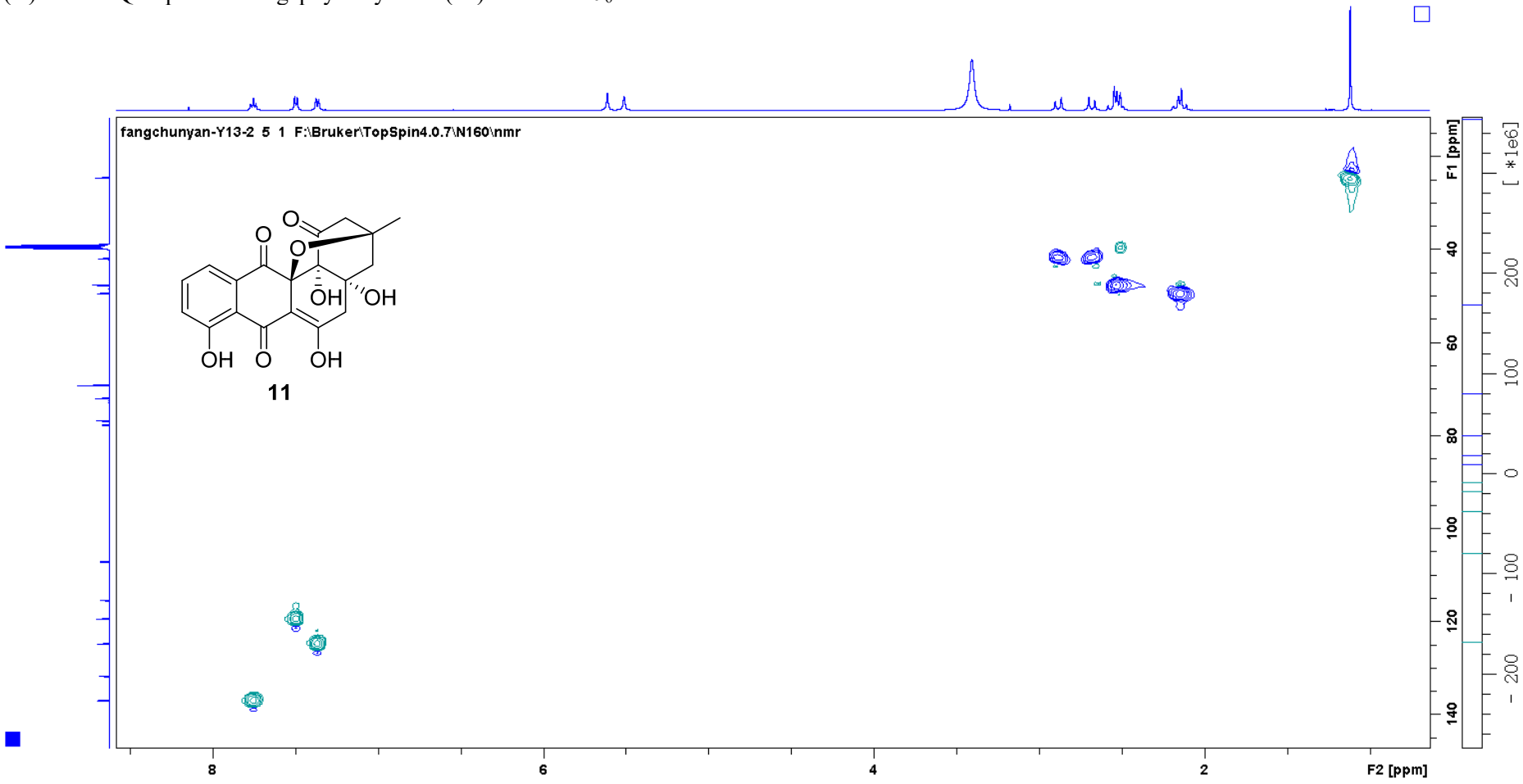

Figure S4. Spectroscopic data for gephyromycin D (**11**). (continued).
(**E**) The COSY spectrum of gephyromycin D (**11**) in DMSO-d_6.

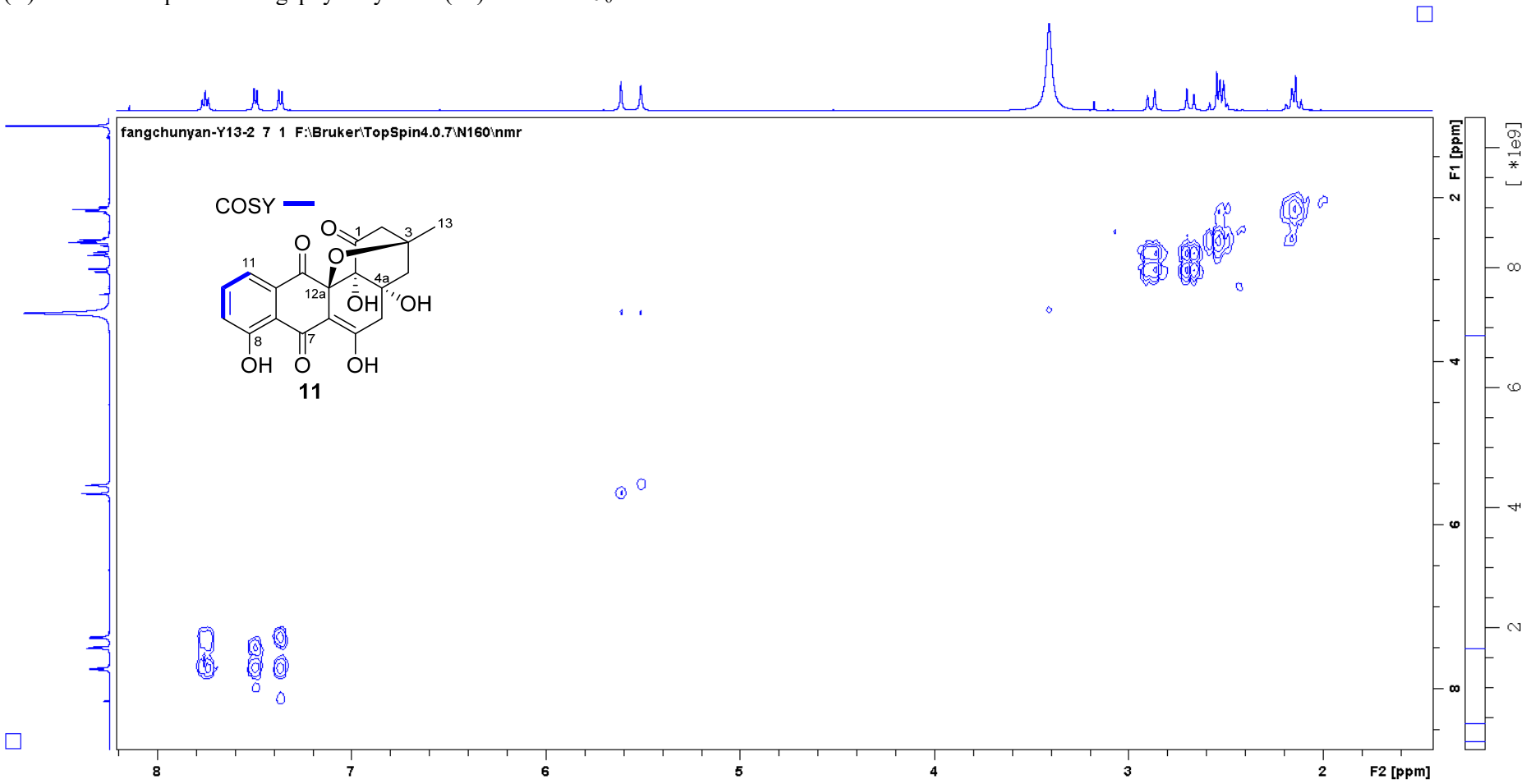

Figure S4. Spectroscopic data for gephyromycin D (**11**). (continued).
(**F**) The HMBC spectrum of gephyromycin D (**11**) in DMSO-d_6.

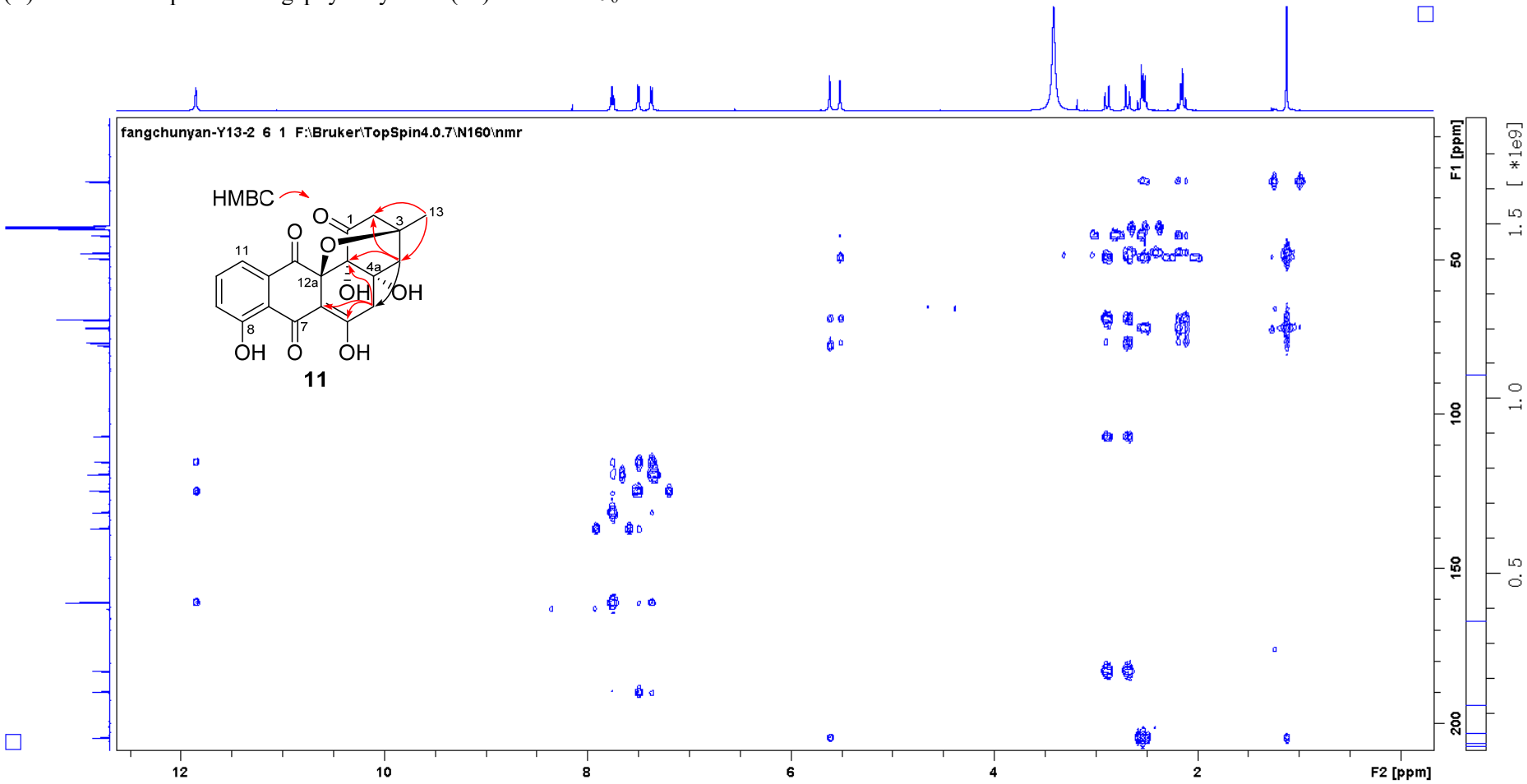

Figure S4. Spectroscopic data for gephyromycin D (**11**). (continued).
(**G**) The NOESY spectrum of gephyromycin D (**11**) in DMSO-d_6.

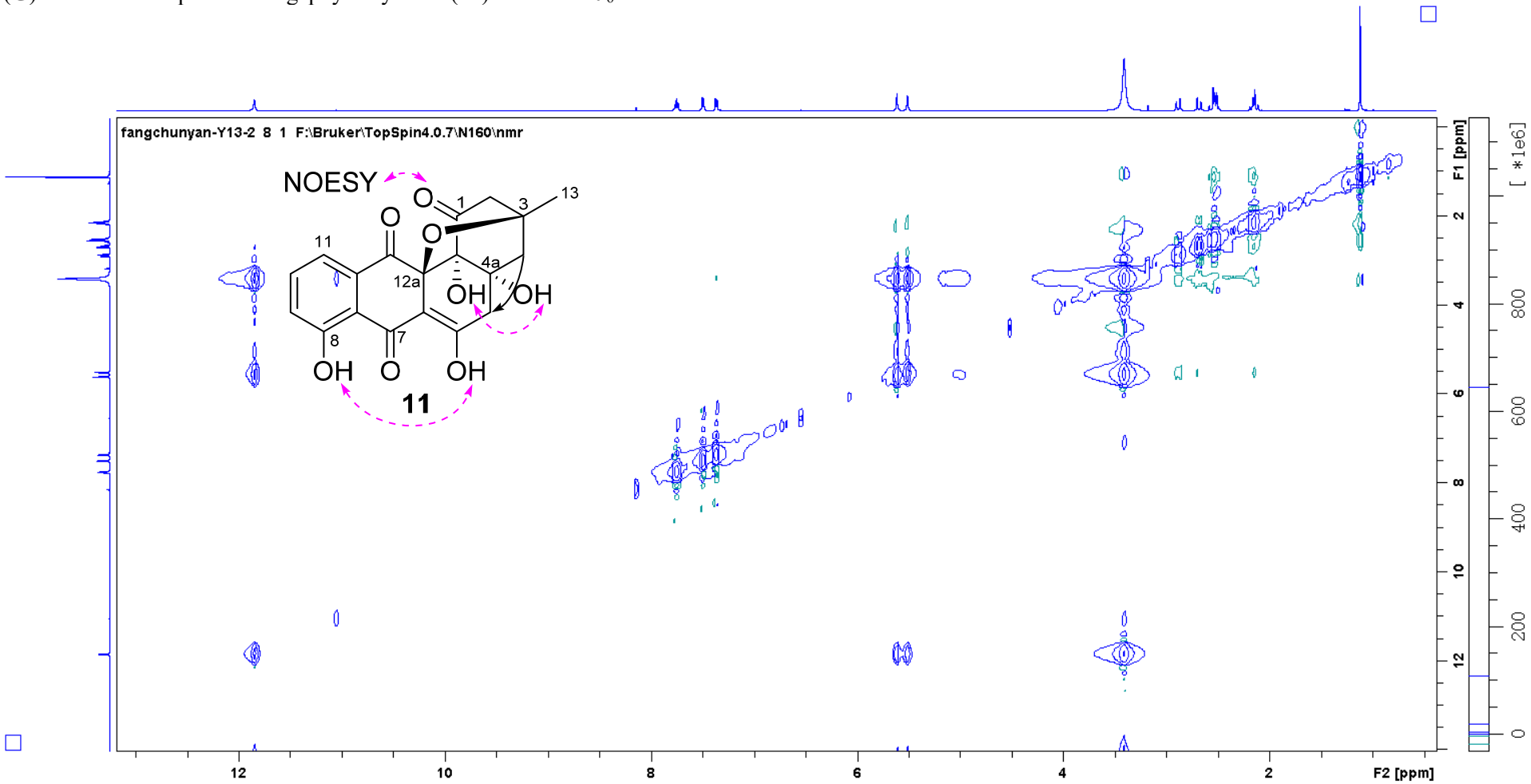

Figure S5. Spectroscopic data for 6-hydroxyfridamycin E (**12**).
(**A**) HRESIMS (**a**), IR (**b**), and UV (**c**) spectra of 6-hydroxyfridamycin E (**12**).
(a) HRESIMS

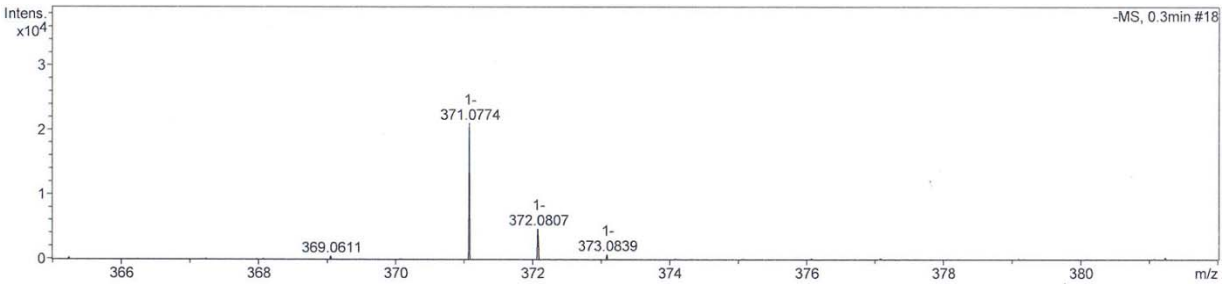

(b) IR.

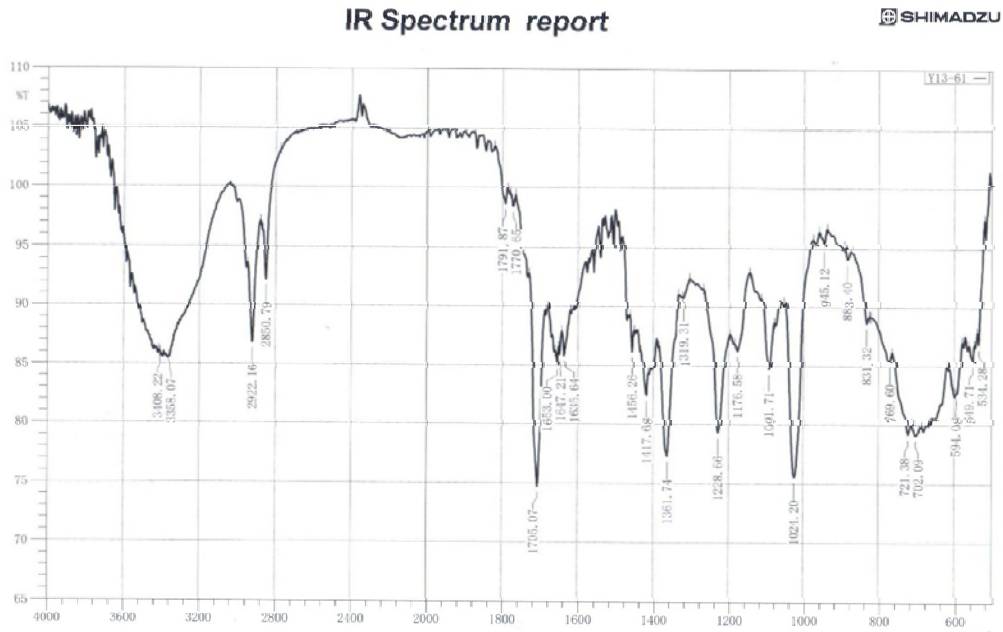

(c) UV.

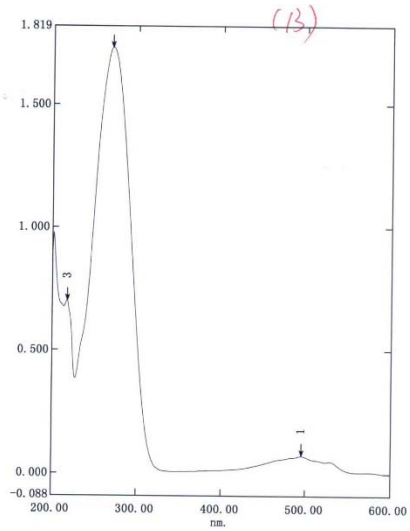

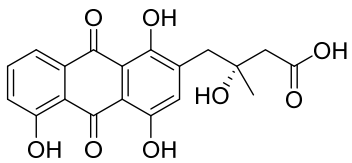

12

Figure S5. Spectroscopic data for 6-hydroxyfridamycin E (**12**). (continued).
(**B**) The ^{1}H NMR spectrum (700 MHz) of 6-hydroxyfridamycin E (**12**) in pyridine-d_5.

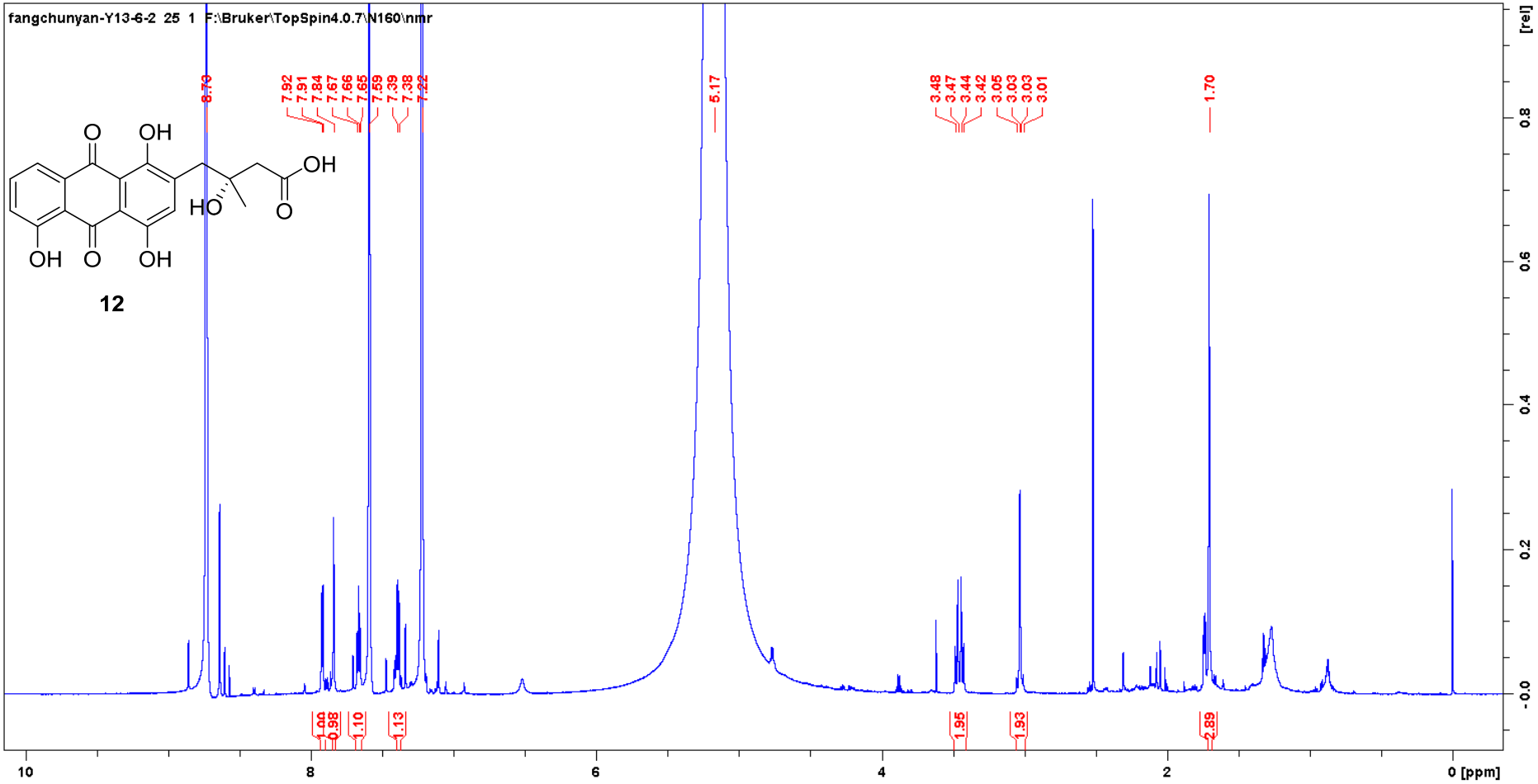

Figure S5. Spectroscopic data for 6-hydroxyfridamycin E (**12**). (continued).
(**C**) The $^{13}C\{^{1}H\}$ NMR spectrum (176 MHz) of 6-hydroxyfridamycin E (**12**) in pyridine-d_5.

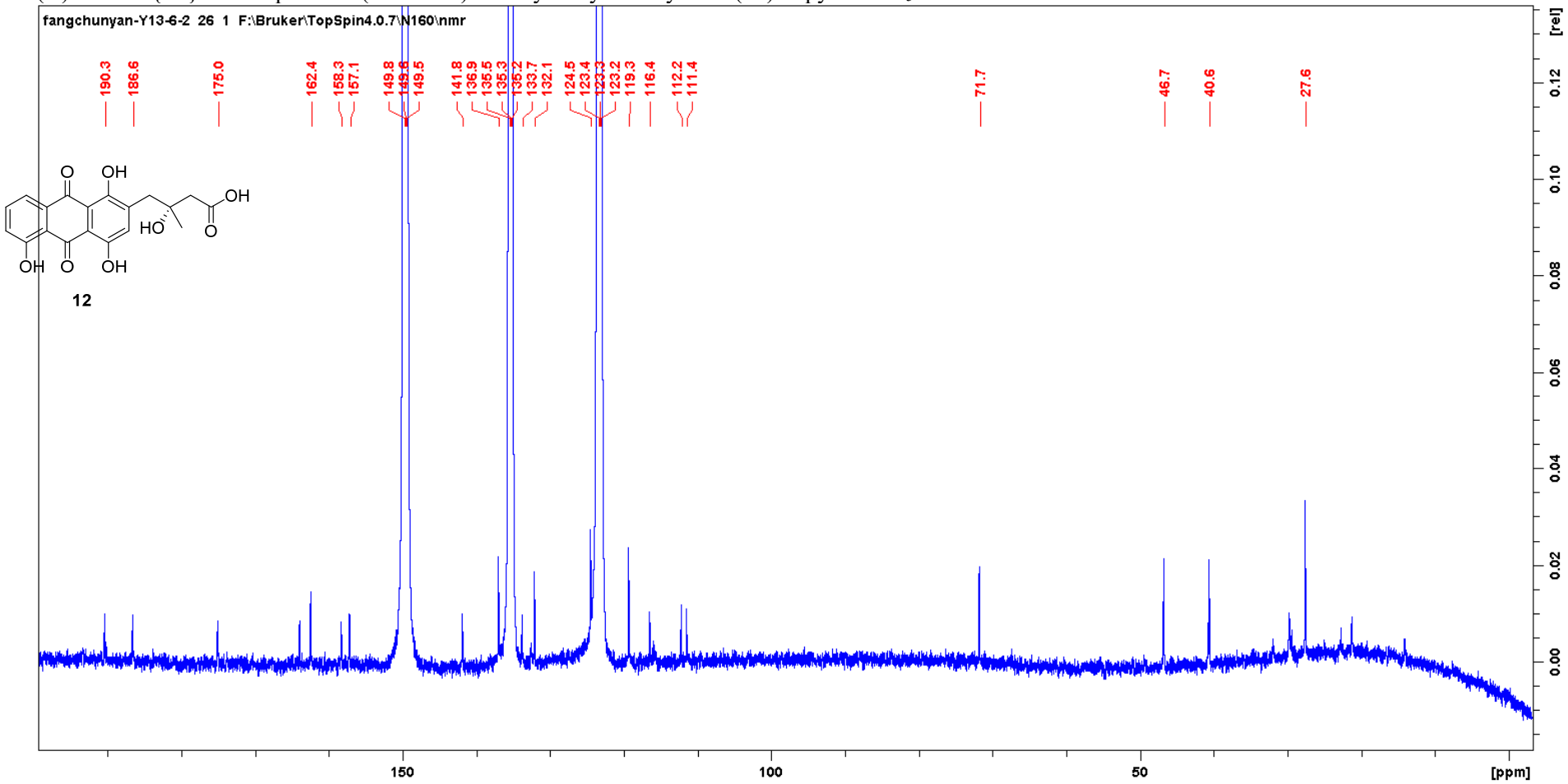

Figure S5. Spectroscopic data for 6-hydroxyfridamycin E (**12**). (continued).
(**D**) The HSQC spectrum of 6-hydroxyfridamycin E (**12**) in pyridine-d_5.

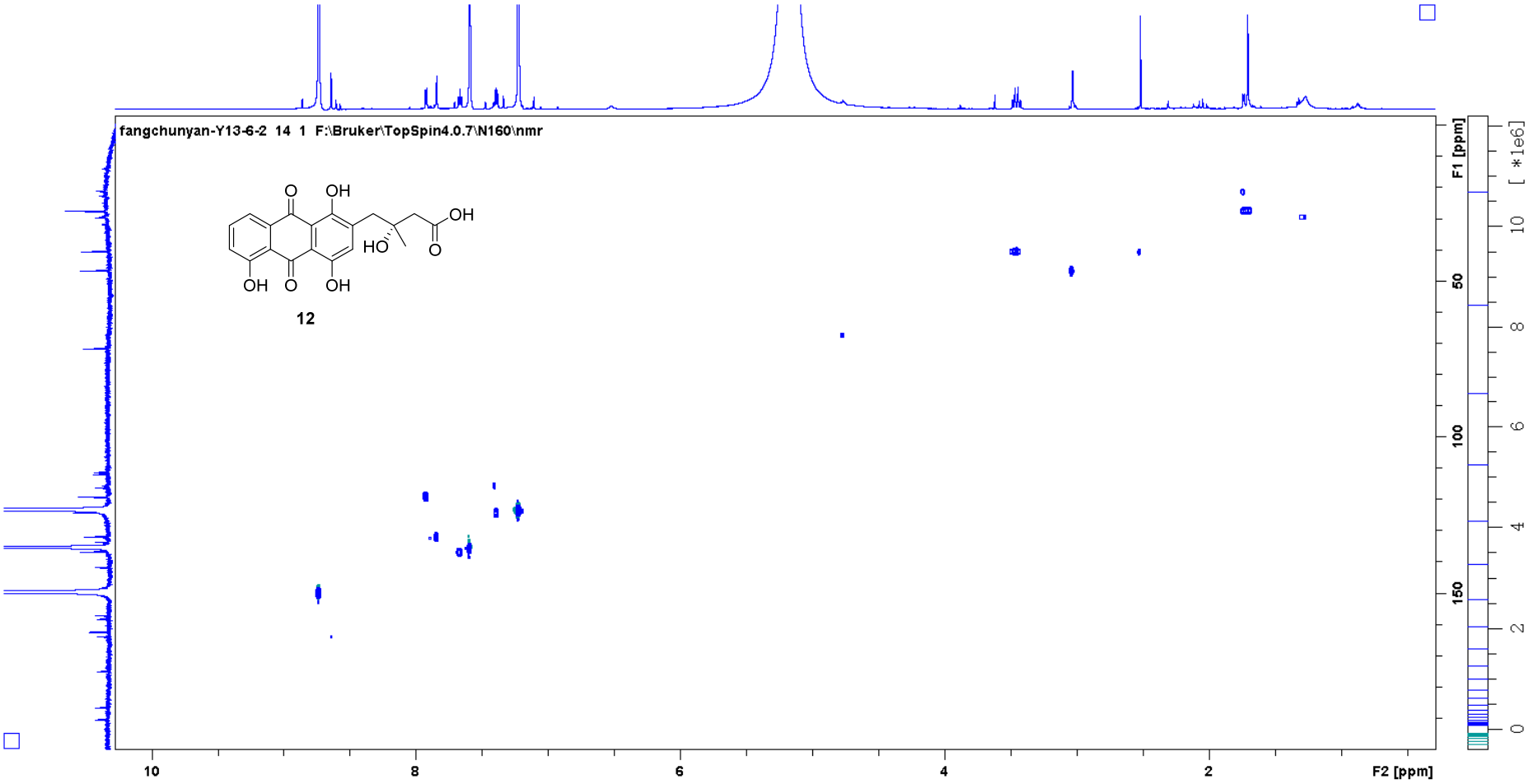

Figure S5. Spectroscopic data for 6-hydroxyfridamycin E (**12**). (continued).
(**E**) The COSY spectrum of 6-hydroxyfridamycin E (**12**) in pyridine-d_5.

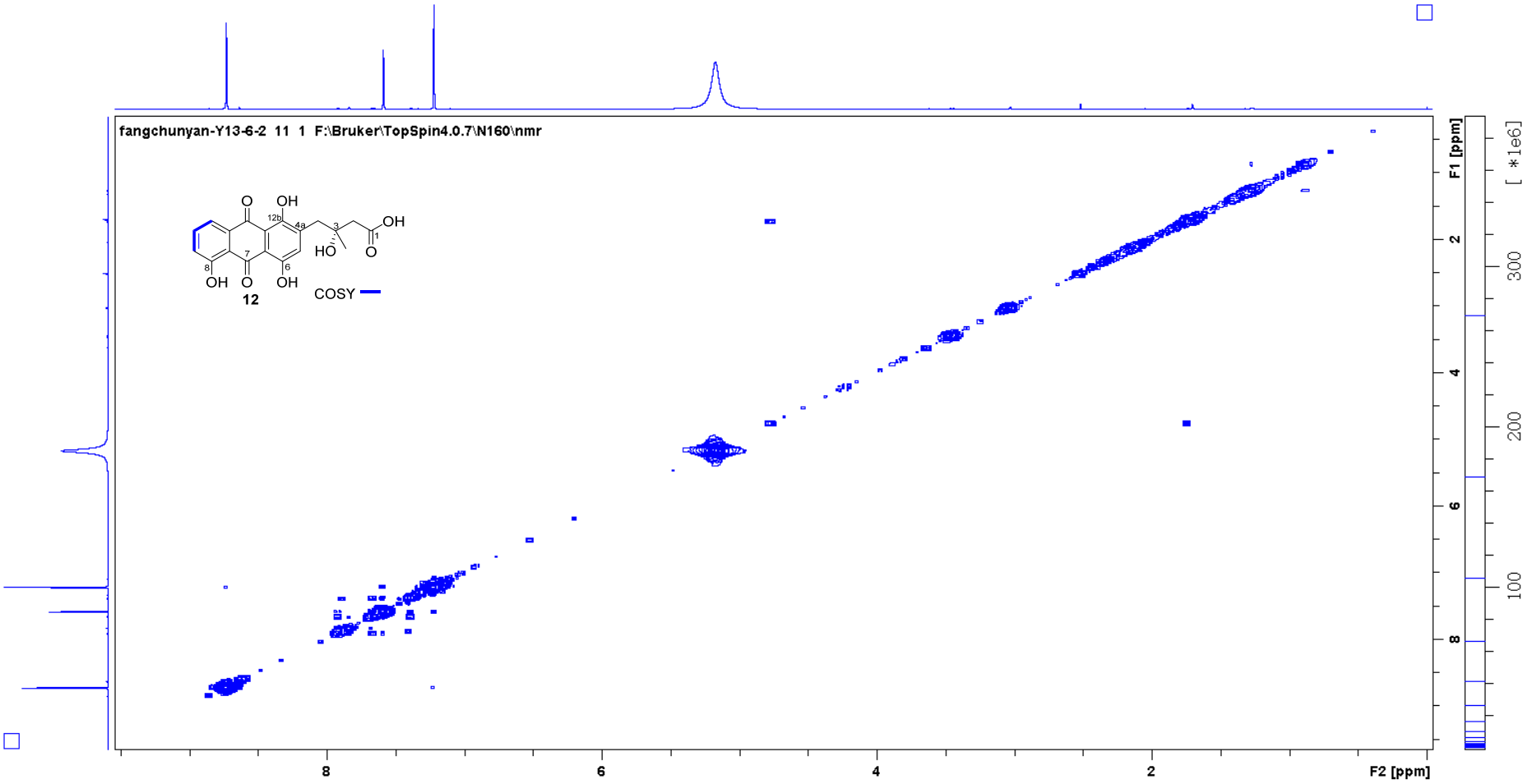

Figure S5. Spectroscopic data for 6-hydroxyfridamycin E (**12**). (continued).
(**F**) The HMBC spectrum of 6-hydroxyfridamycin E (**12**) in pyridine-d_5.

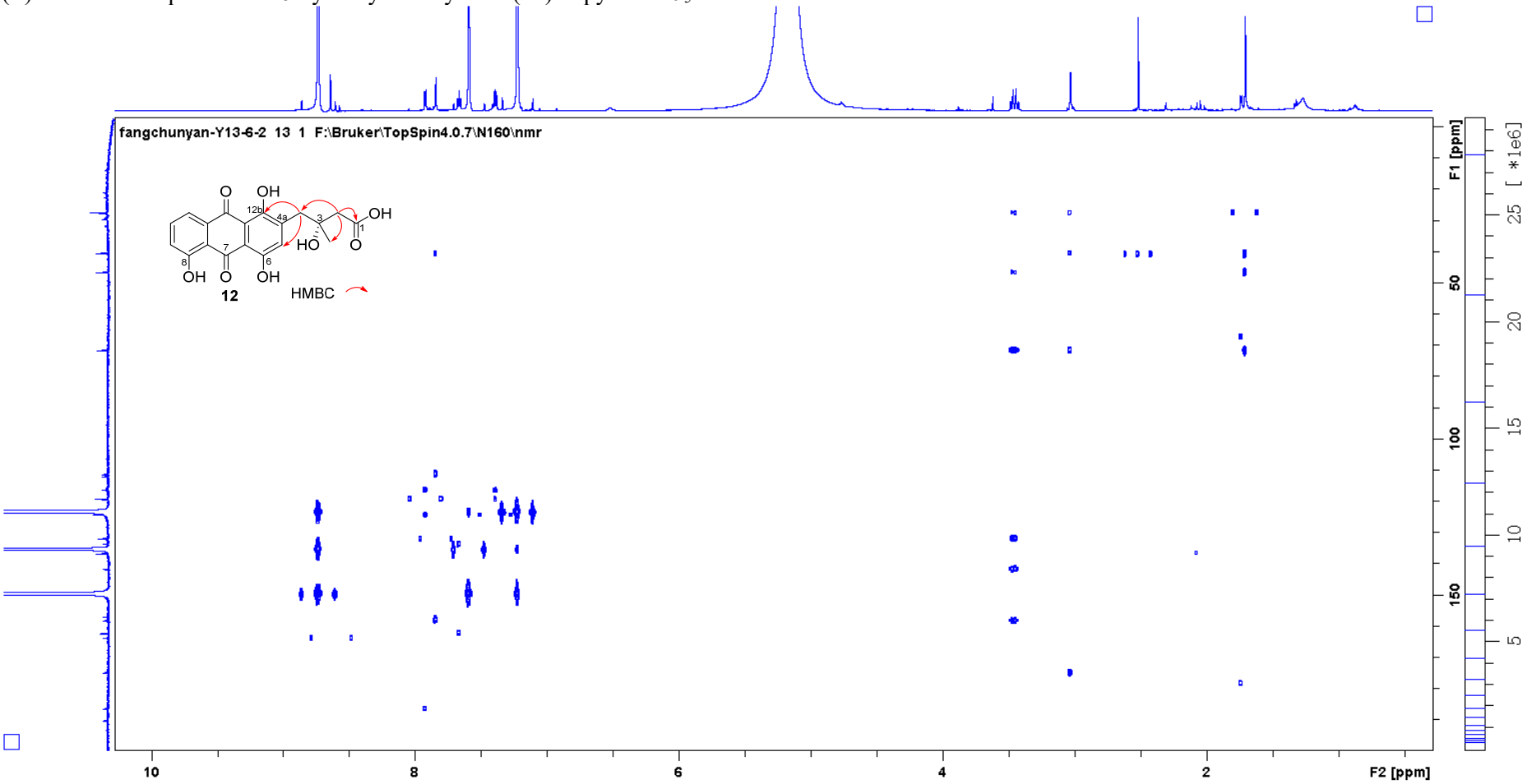

Figure S6. Spectroscopic data for PK1 (**16**).
(**A**) HRESIMS (**a**), IR (**b**), and UV (**c**) spectra of PK1 (**16**).
(a) HRESIMS

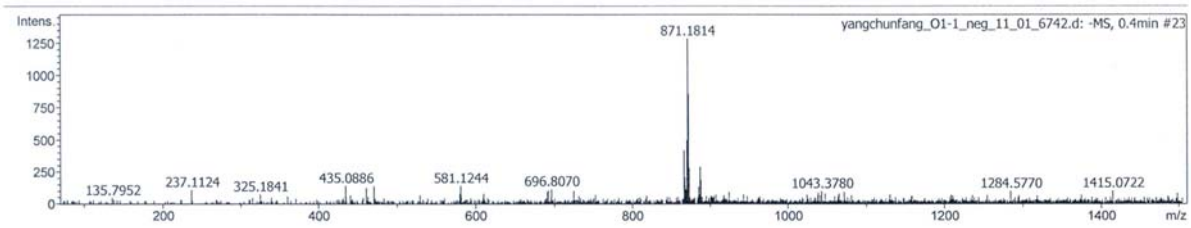

(b) IR.

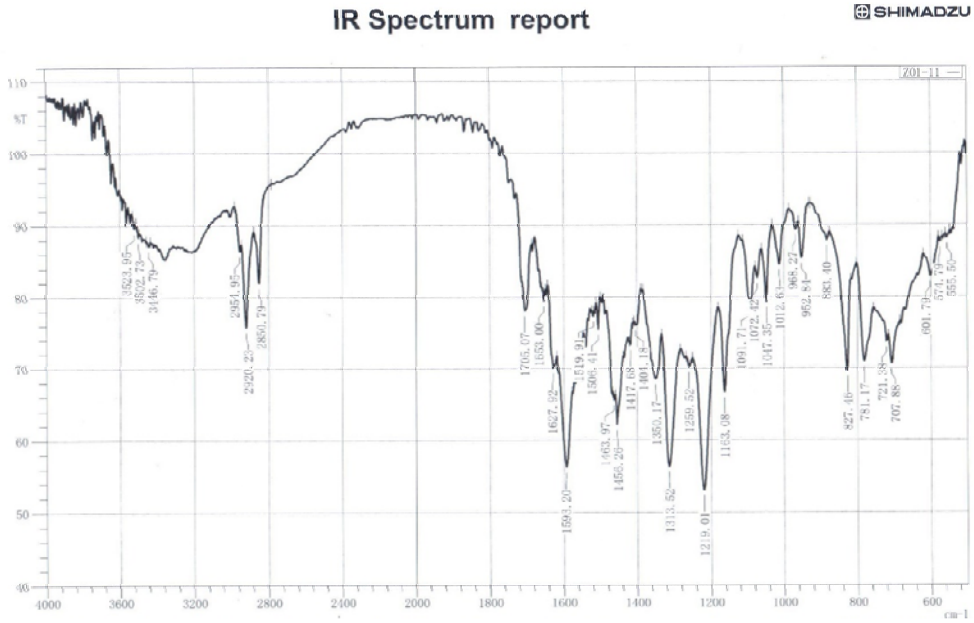

(c) UV.

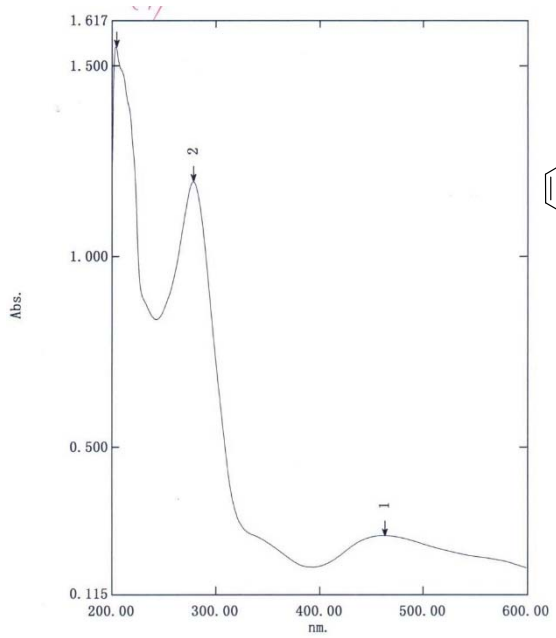

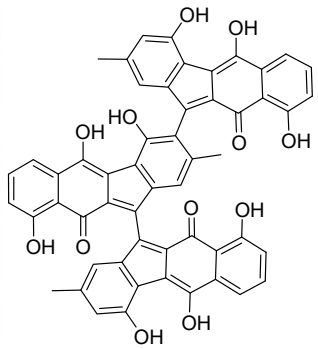

Figure S6. Spectroscopic data for PK1 (**16**). (continued).
(B) The ^{1}H NMR spectrum (700 MHz) of PK1 (**16**) in DMSO-d_6.

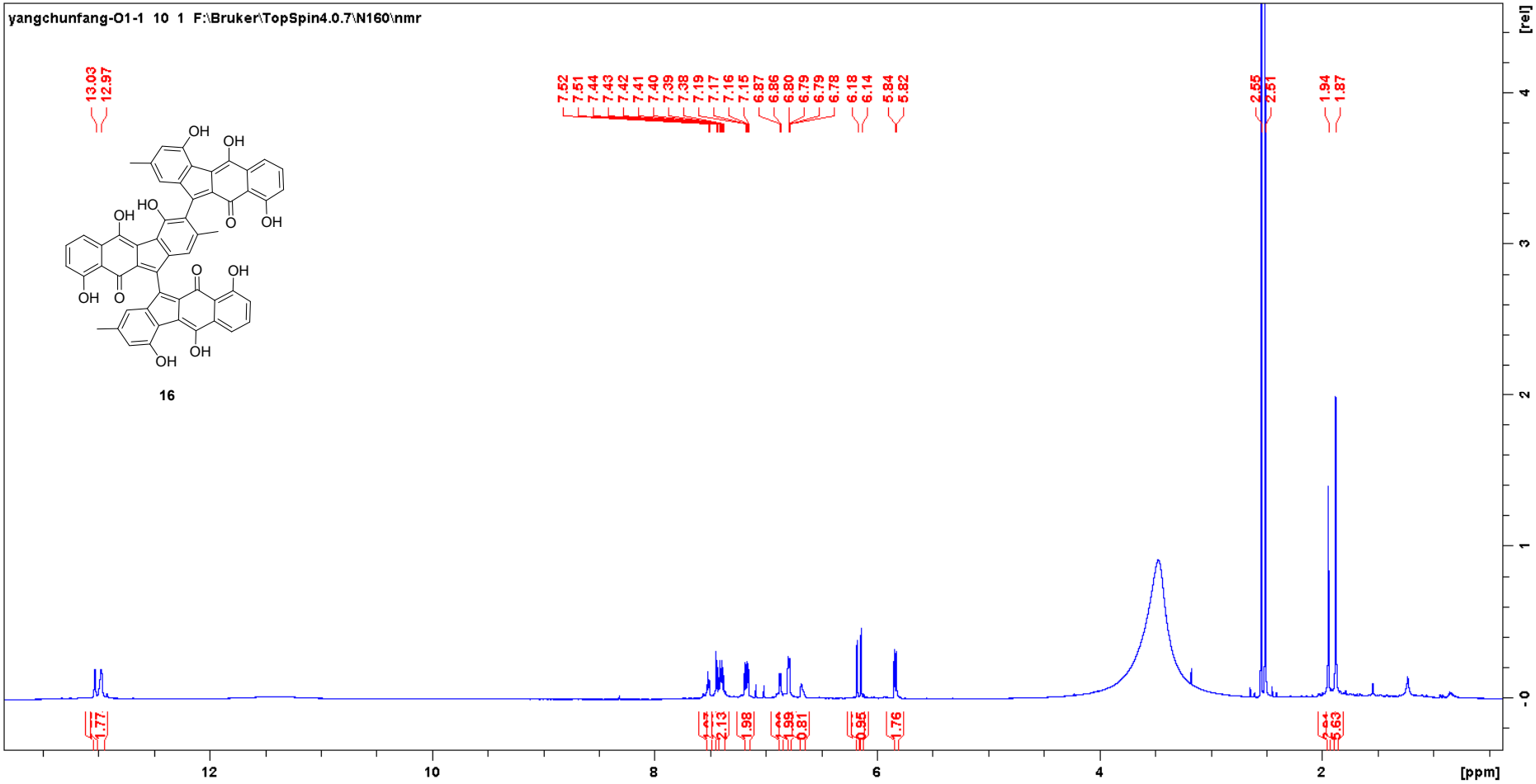

Figure S6. Spectroscopic data for PK1 (**16**). (continued).
(C) The ^{1}H NMR spectrum (5.0 – 8.0 ppm) (700 MHz) of PK1 (**16**) in DMSO-d_6.

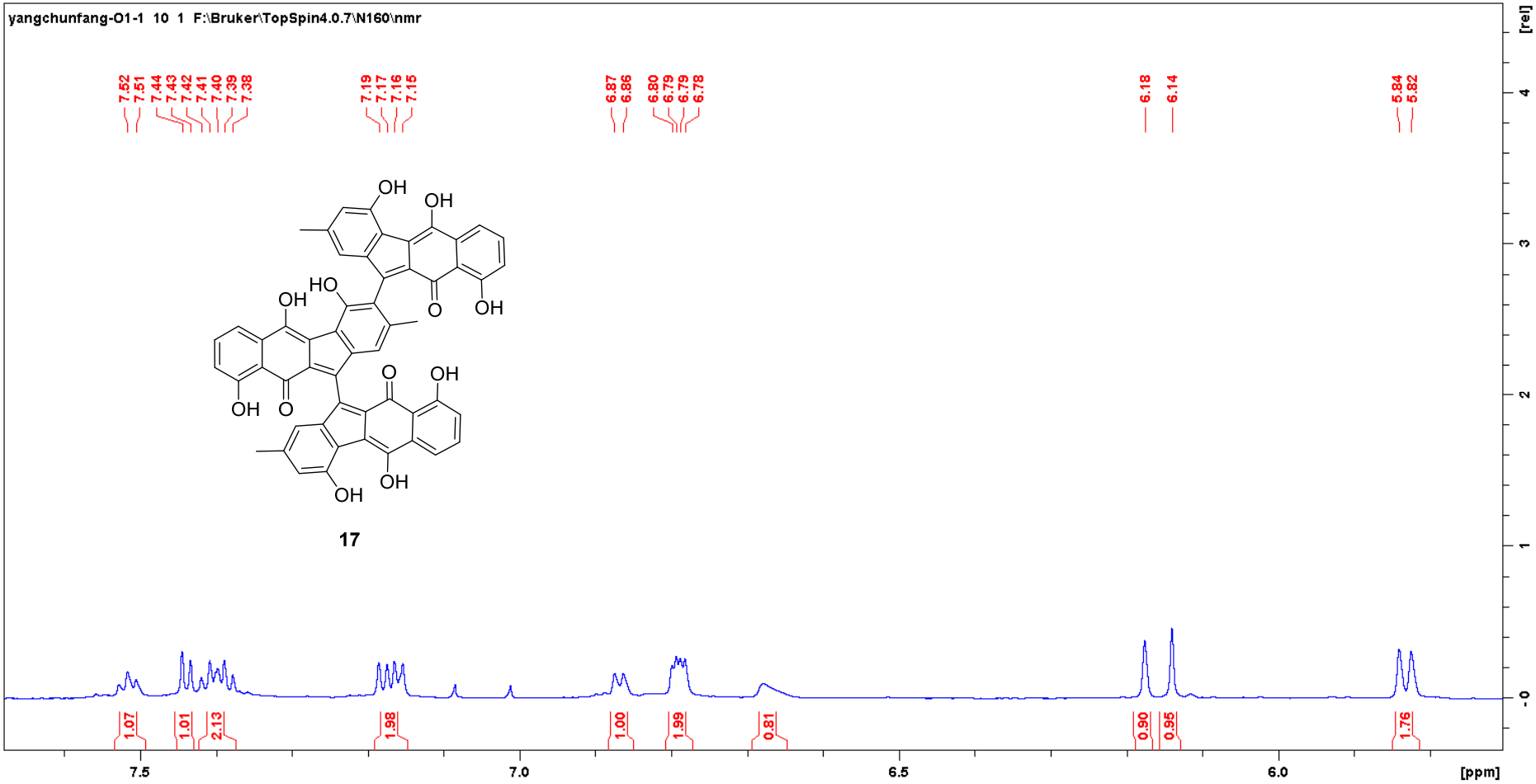

Figure S6. Spectroscopic data for PK1 (**16**). (continued).
(D) The $^{13}C\{^{1}H\}$ and DEPT 135 NMR spectrum (176 MHz) of PK1 (**16**) in DMSO-d_6.

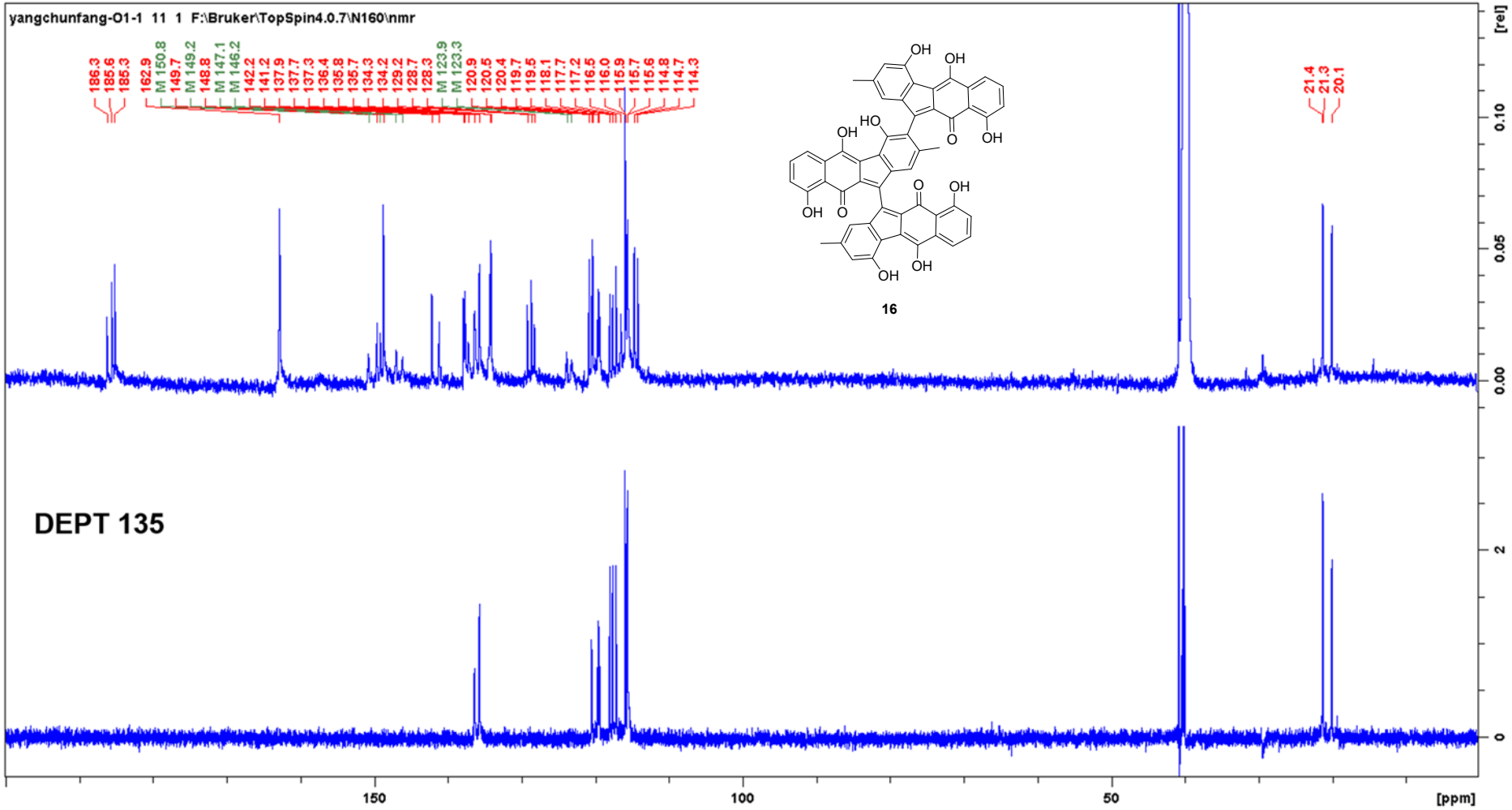

Figure S6. Spectroscopic data for PK1 (**16**). (continued).
(E) The $^{13}C\{^{1}H\}$ (112-154 ppm) spectrum (176 MHz) of PK1 (**16**) in DMSO-d_6.

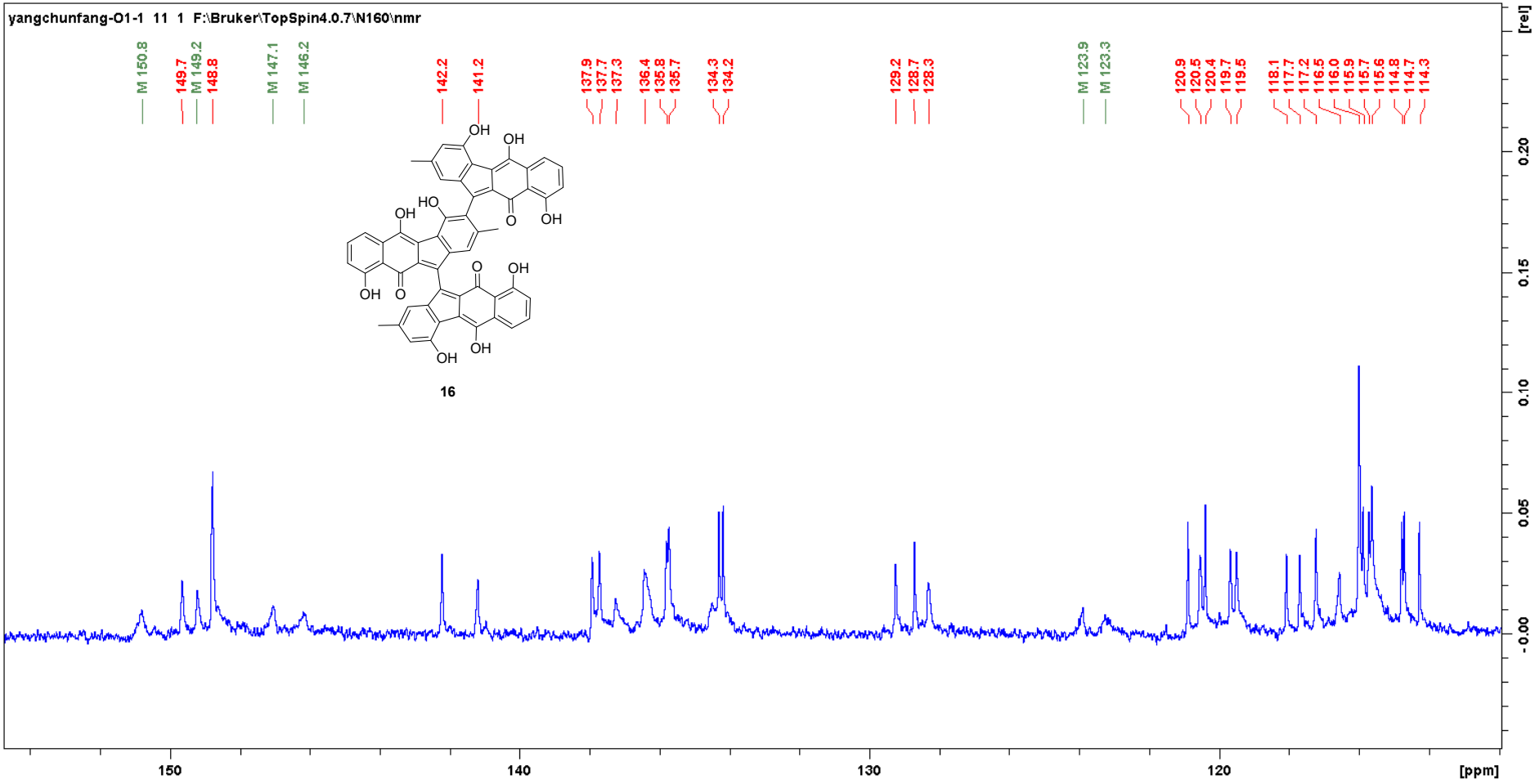

Figure S7. Spectroscopic data for fluostarene A (**14**).

(A) HRESIMS (a), IR (b), and UV (c) spectra of fluostarene A (**14**)

(a) HRESIMS

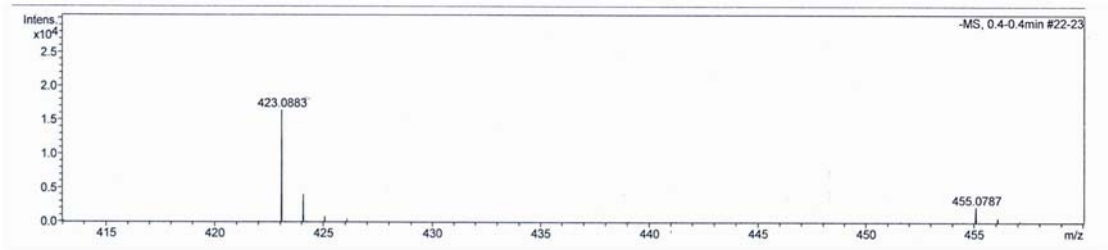

(b) IR.

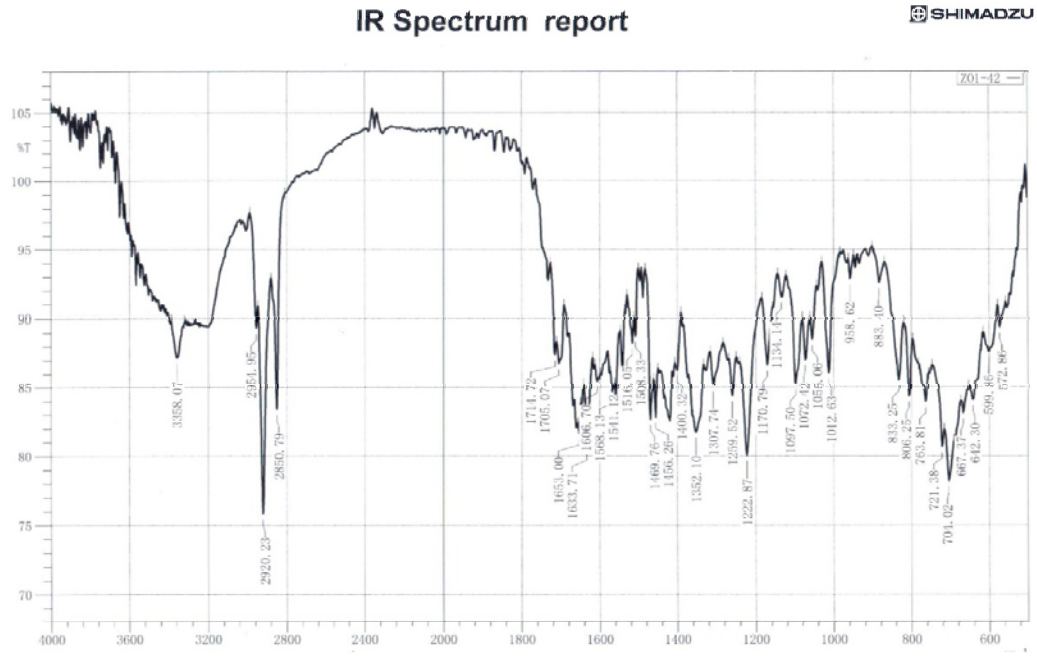

(c) UV.

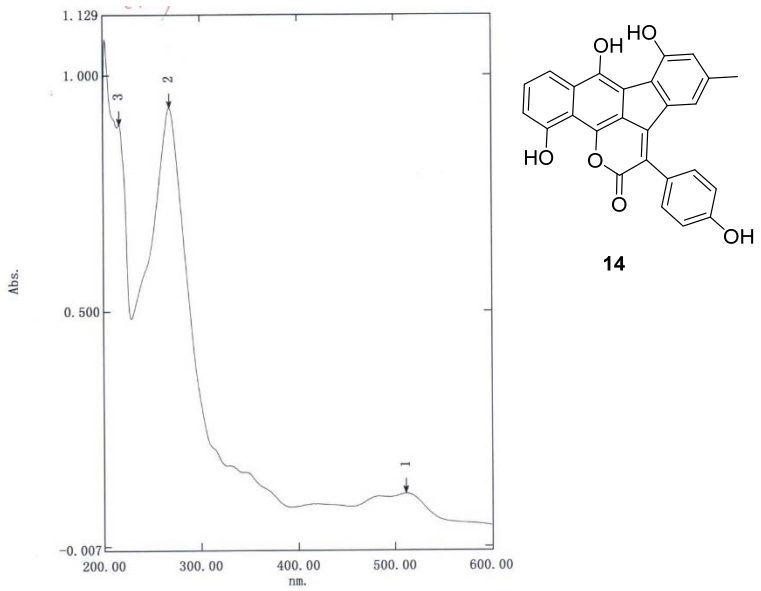

Figure S7. Spectroscopic data for fluostarene A (**14**). (continued).
(B) The ^{1}H NMR spectrum (700 MHz) of fluostarene A (**14**) in DMSO-d_6.

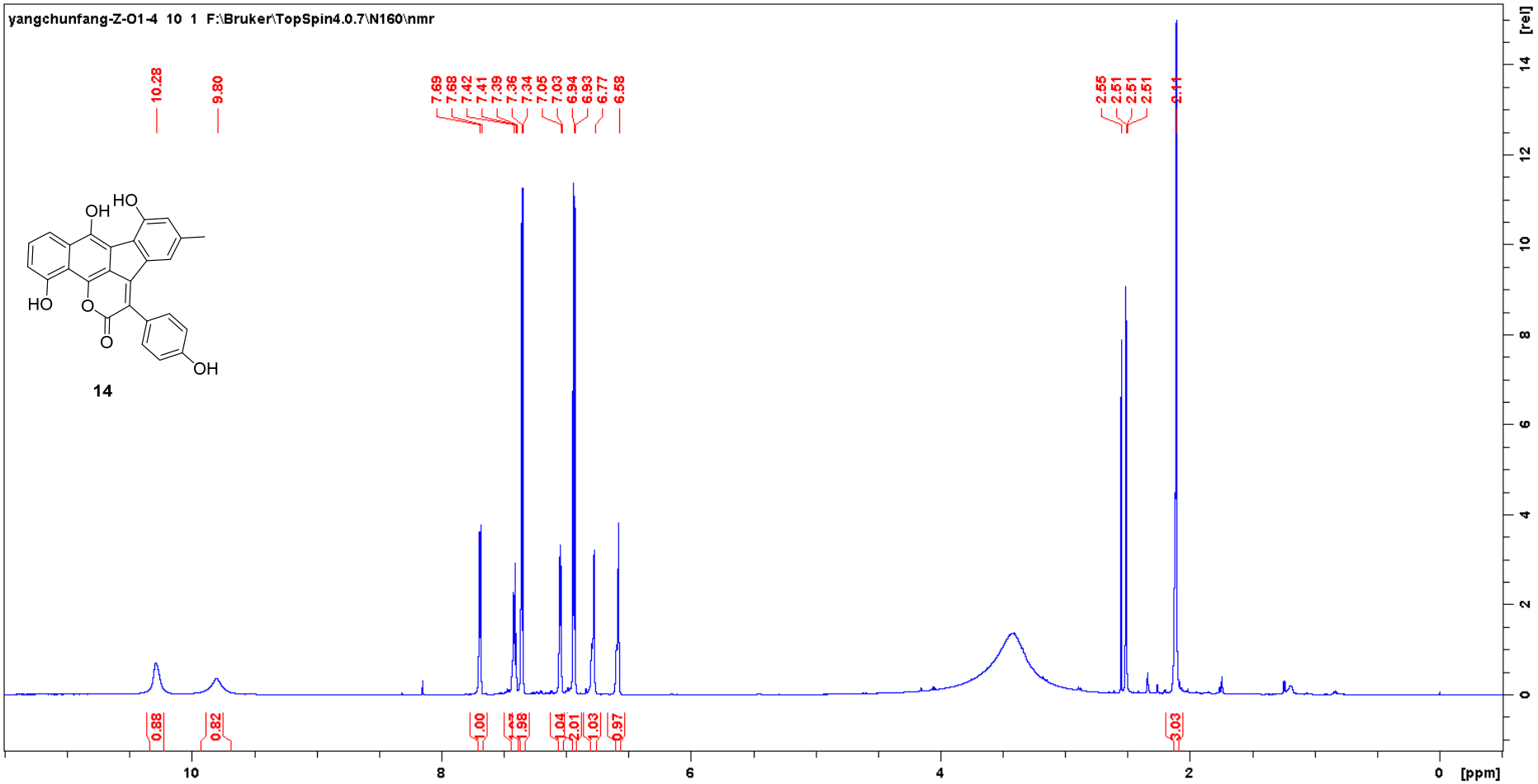

Figure S7. Spectroscopic data for fluostarene A (**14**). (continued).

(C) The $^{13}C\{^{1}H\}$ and DEPT 135 NMR spectrum (176 MHz) of fluostarene A (**14**) in DMSO-d_6.

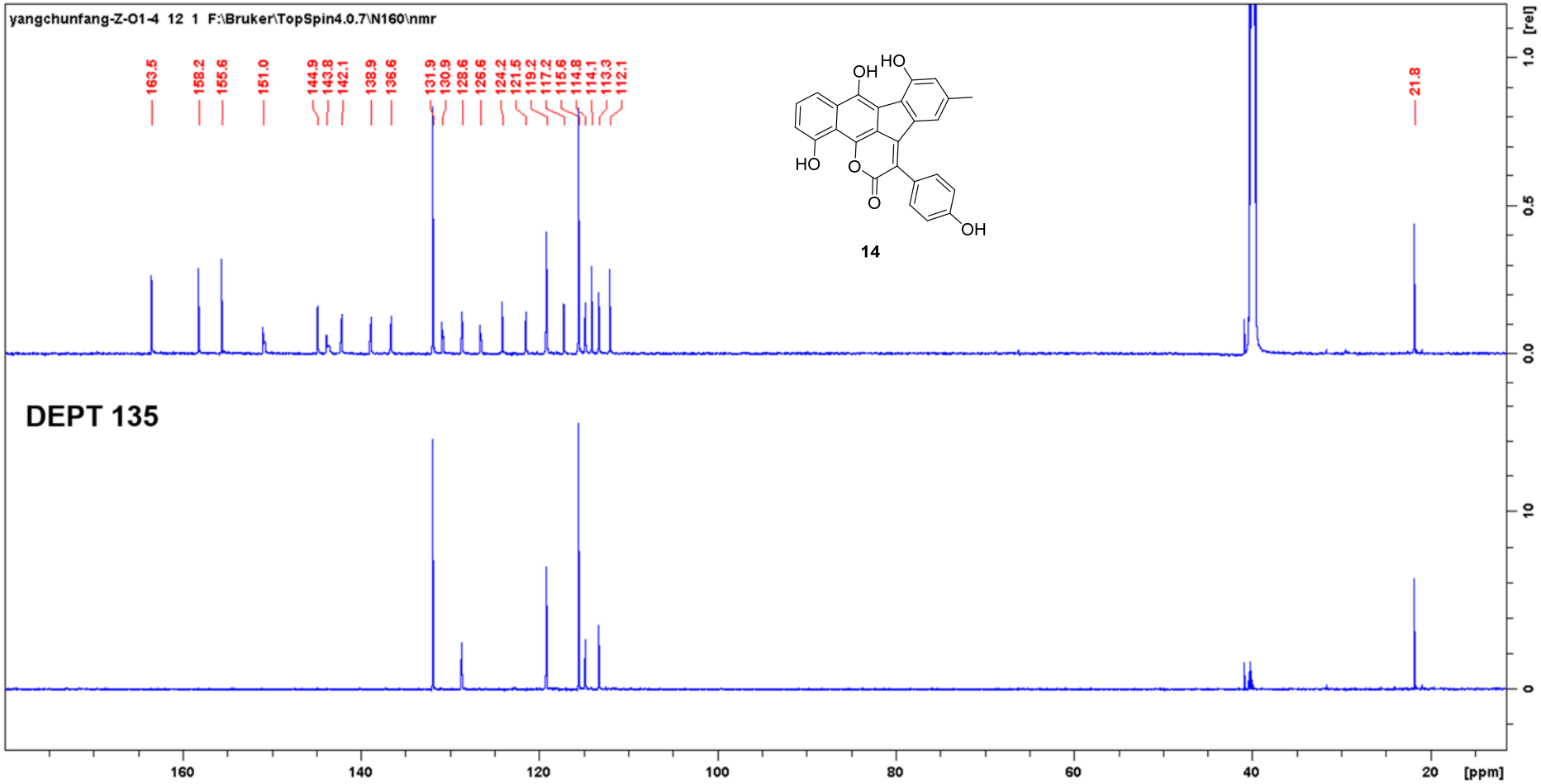

Figure S7. Spectroscopic data for fluostarene A (**14**). (continued).
(D) The HSQC spectrum of fluostarene A (**14**) in DMSO-d_6.

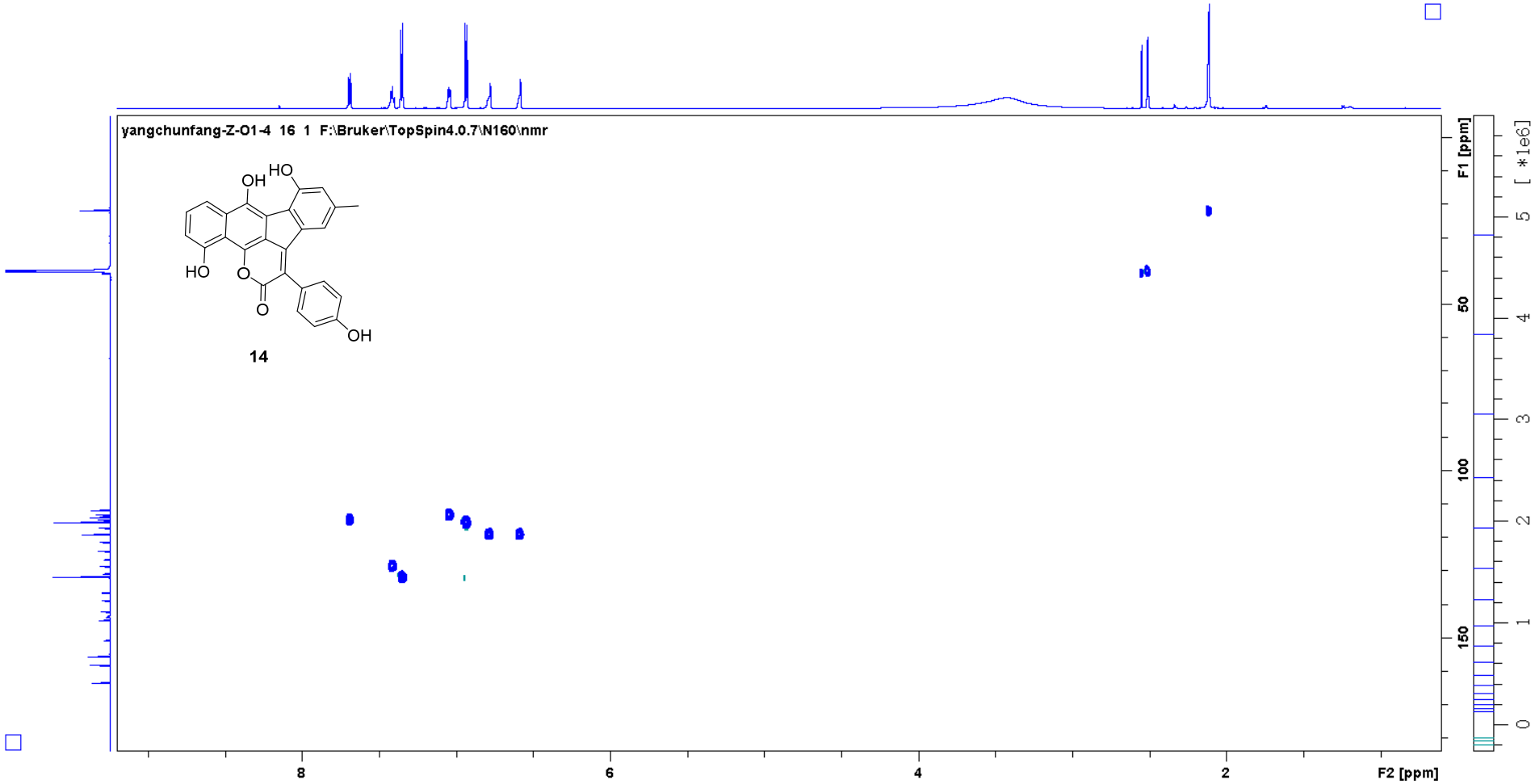

Figure S7. Spectroscopic data for fluostarene A (**14**). (continued).

(E) The COSY spectrum of fluostarene A (**14**) in DMSO-d_6.

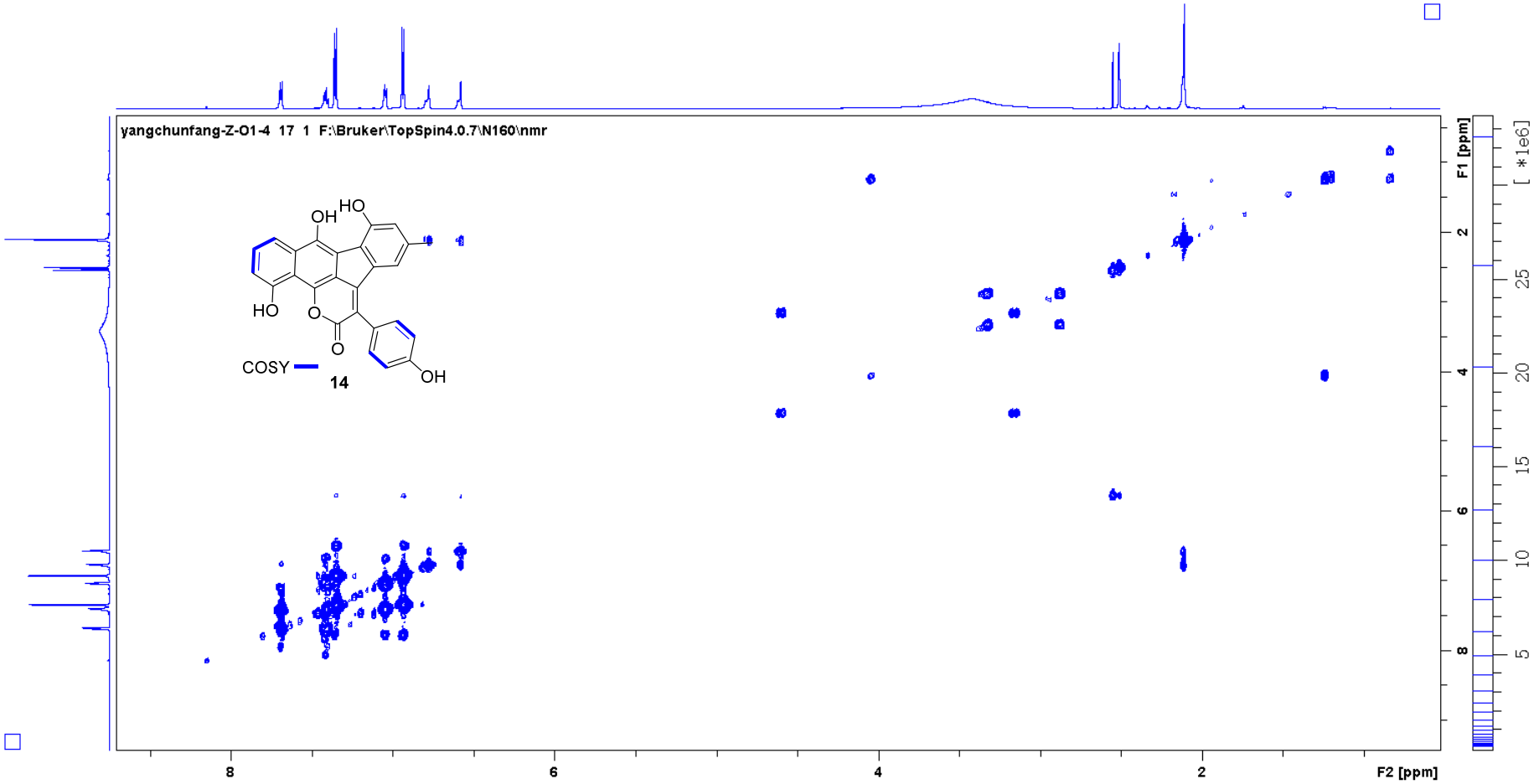

Figure S7. Spectroscopic data for fluostarene A (**14**). (continued).

(F) The HMBC spectrum of fluostarene A (**14**) in DMSO-d_6.

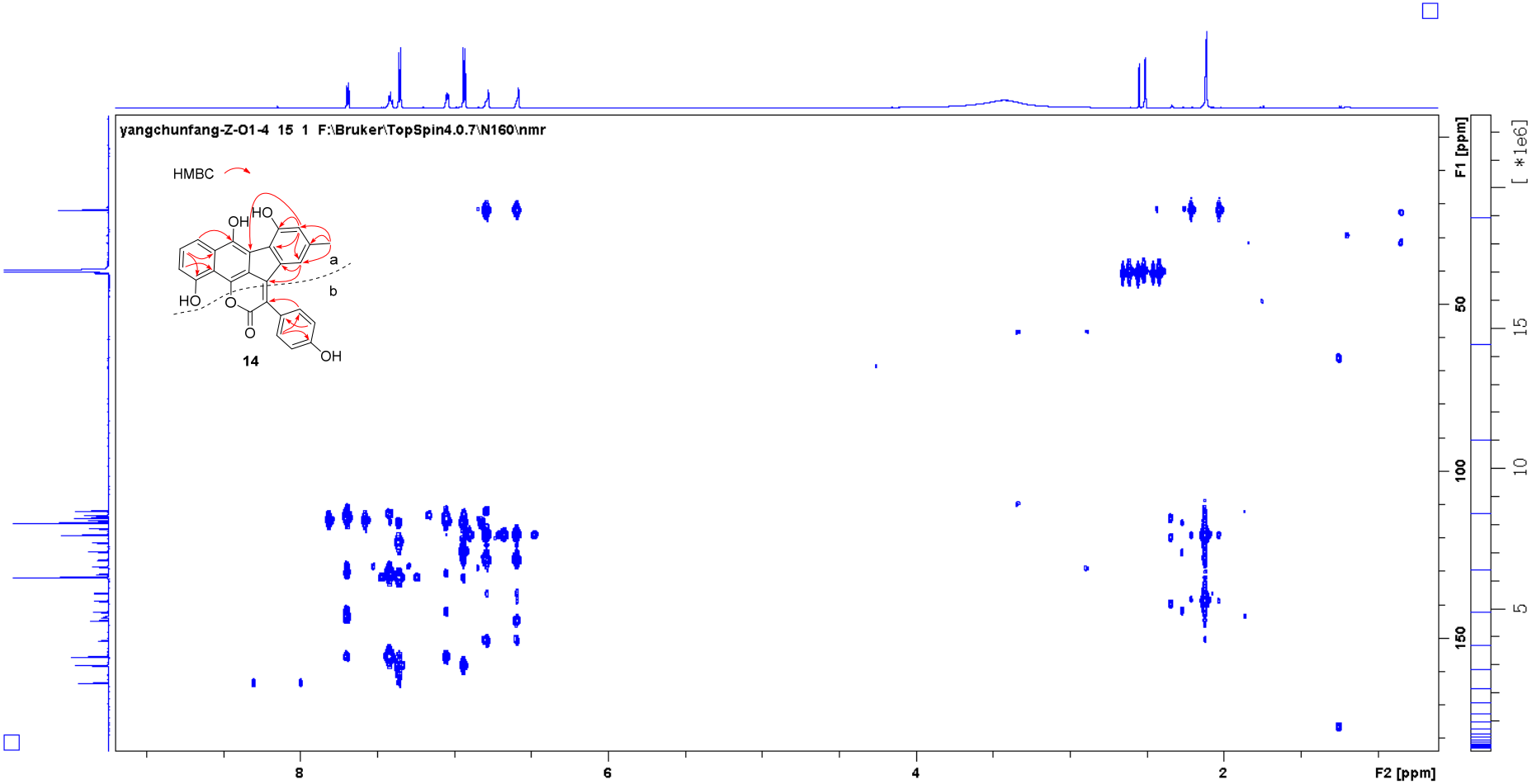

Figure S8. Spectroscopic data for fluostarene B (**15**).
(A) HRESIMS (a), IR (b), and UV (c) spectra of fluostarene B (**15**)
(a) HRESIMS

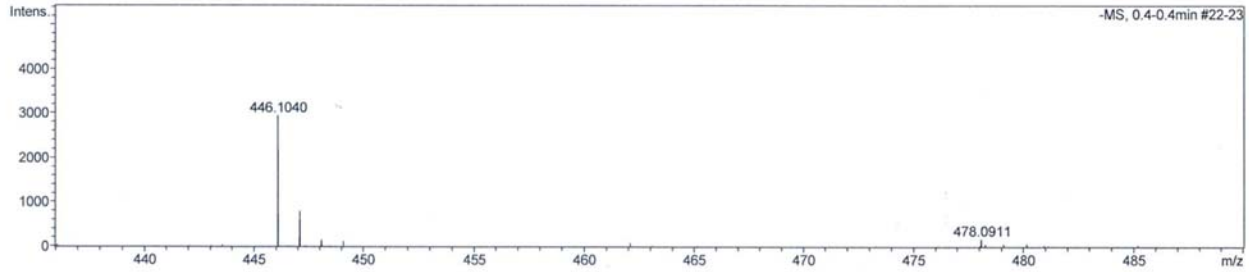

(b) IR.

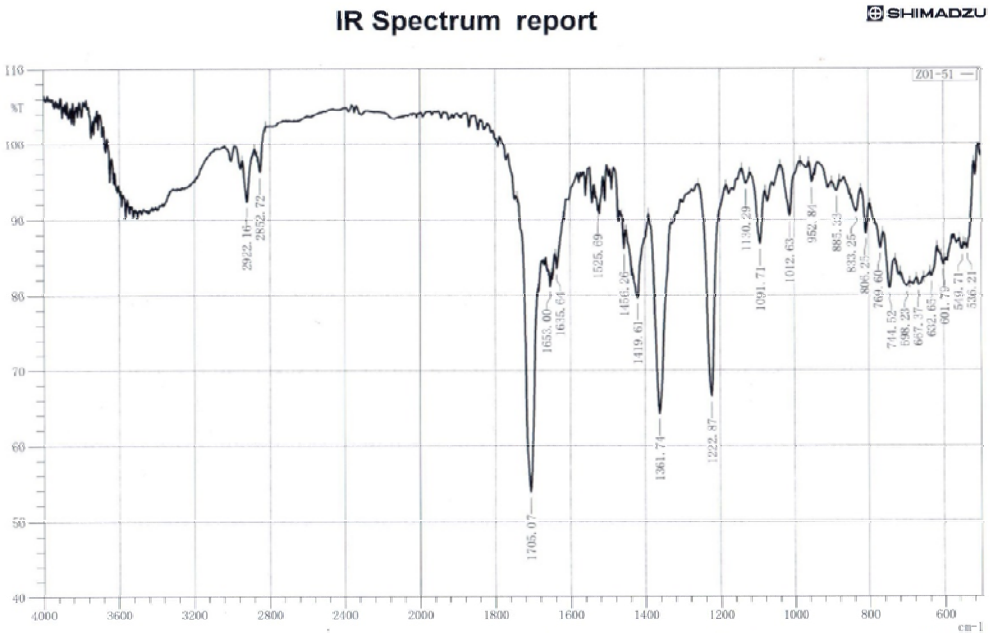

(c) UV.

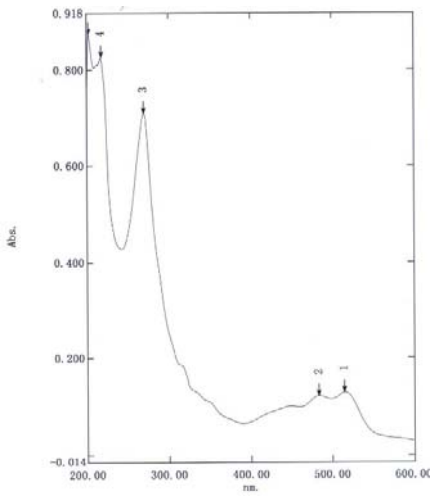

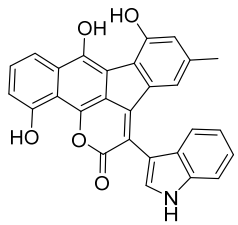

15

Figure S8. Spectroscopic data for fluostarene B (**15**). (continued).
(B) The ^{1}H NMR spectrum (700 MHz) of fluostarene B (**15**) in DMSO-d_6.

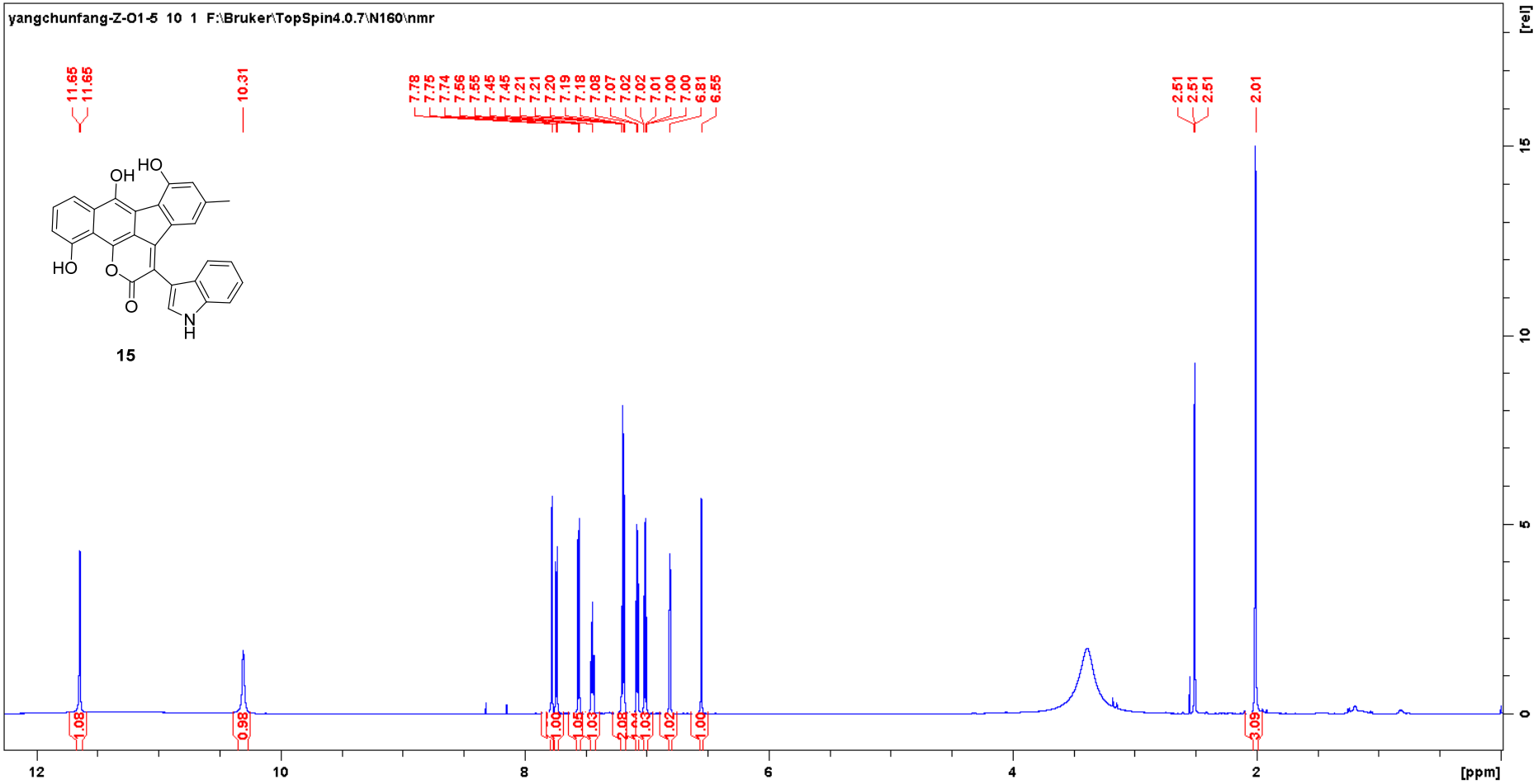

Figure S8. Spectroscopic data for fluostarene B (**15**). (continued).
(C) The ^{1}H NMR (6.3-7.9 ppm) spectrum (176 MHz) of fluostarene B (**15**) in DMSO-d_6.

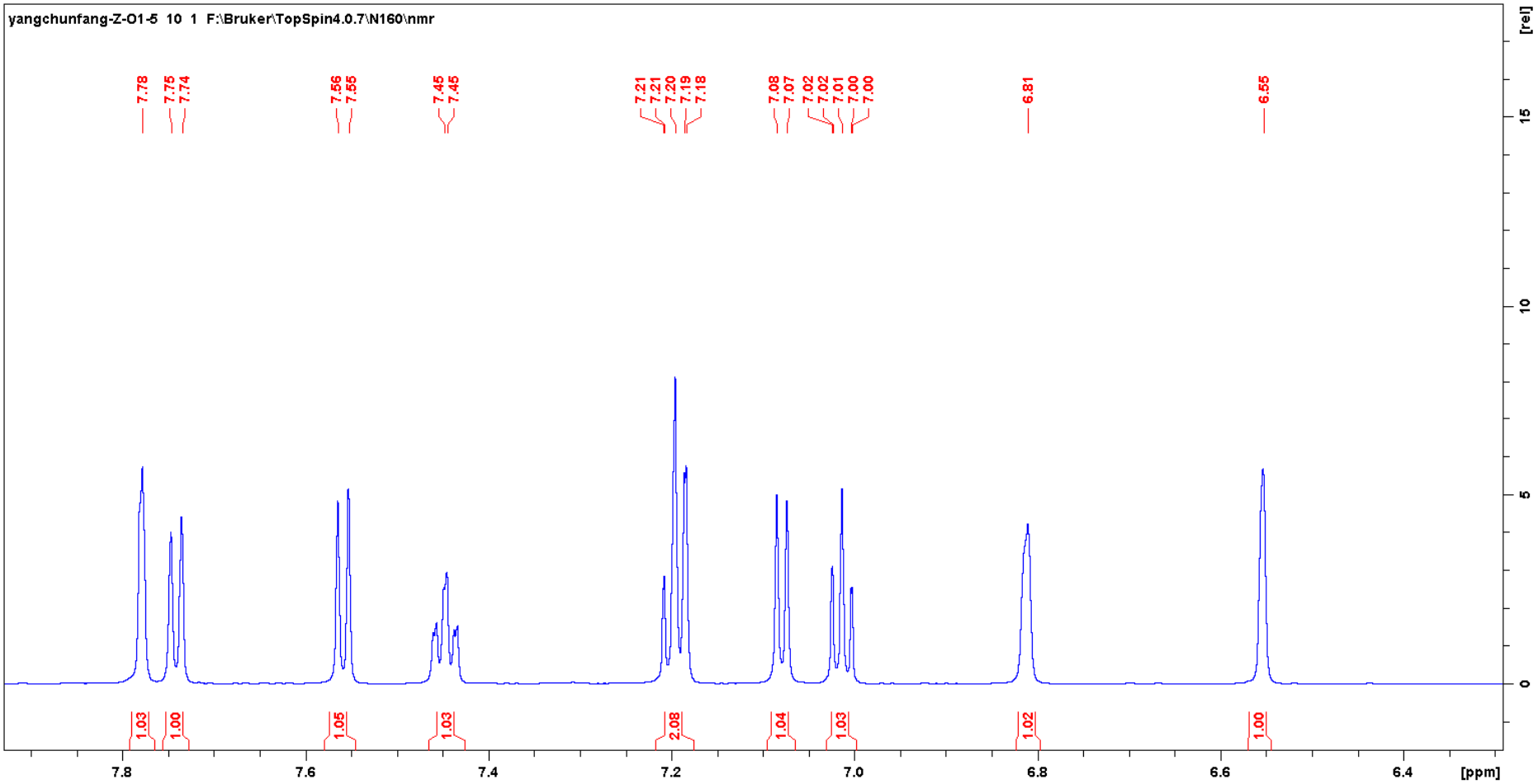

Figure S8. Spectroscopic data for fluostarene B (**15**). (continued).
(D) The^{13}C{^{1}H} NMR and DEPT 135 spectrum (176 MHz) of fluostarene B (**15**) in DMSO-d_6.

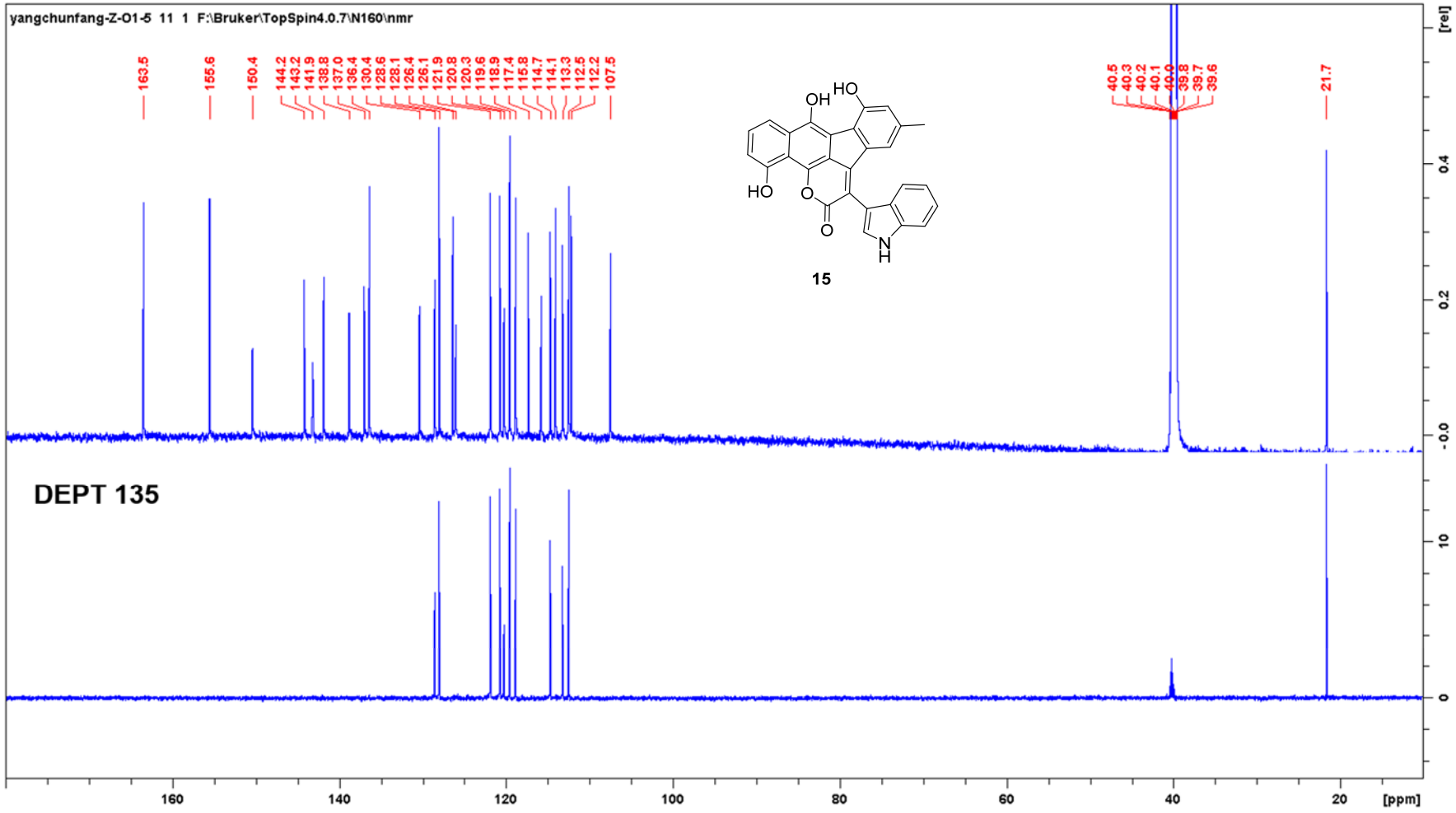

Figure S8. Spectroscopic data for fluostarene B (**15**). (continued).

(E) The HSQC spectrum of fluostarene B (**15**) in DMSO-d_6.

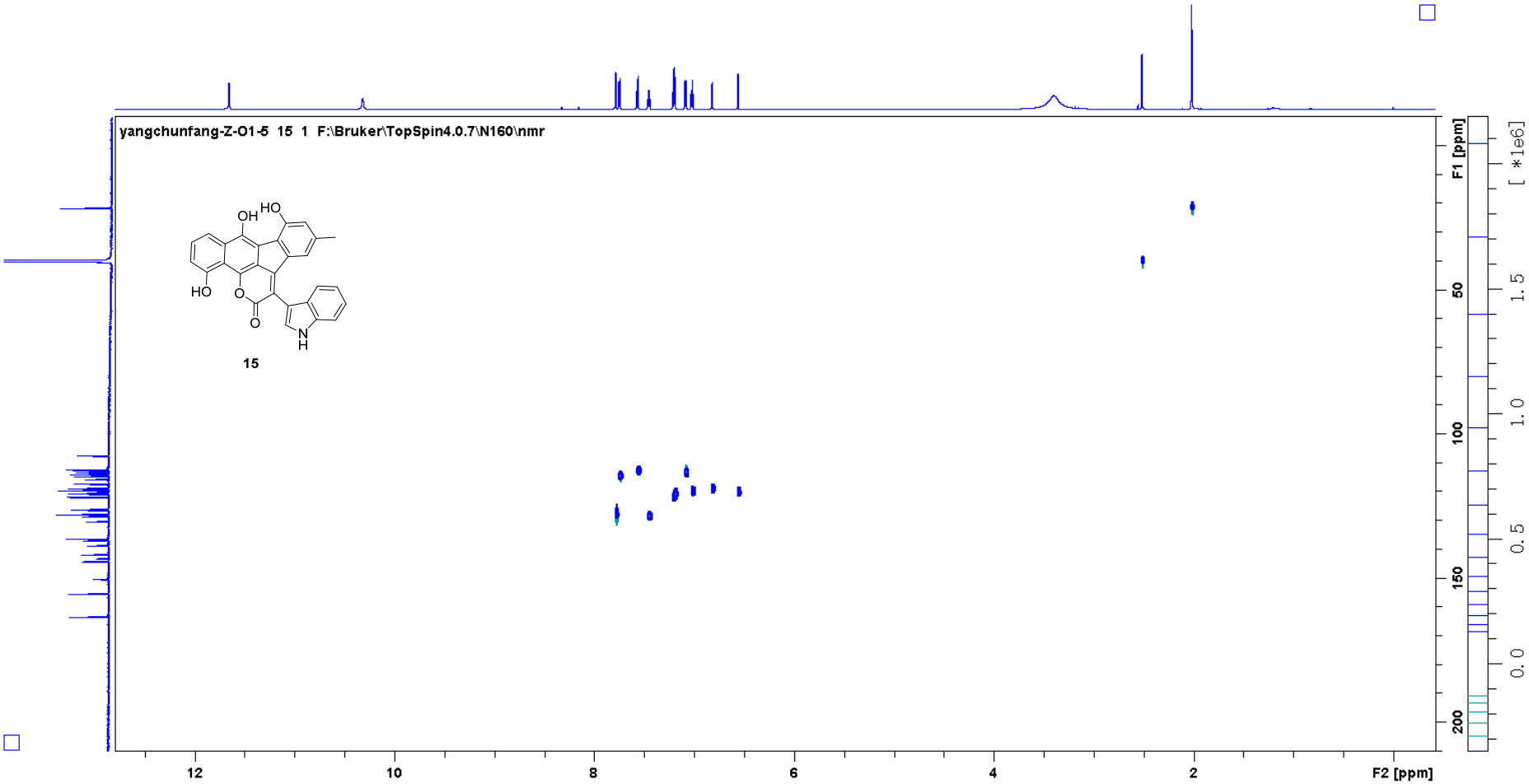

Figure S8. Spectroscopic data for fluostarene B (**15**). (continued).

(F) The COSY spectrum of fluostarene B (**15**) in DMSO-d_6.

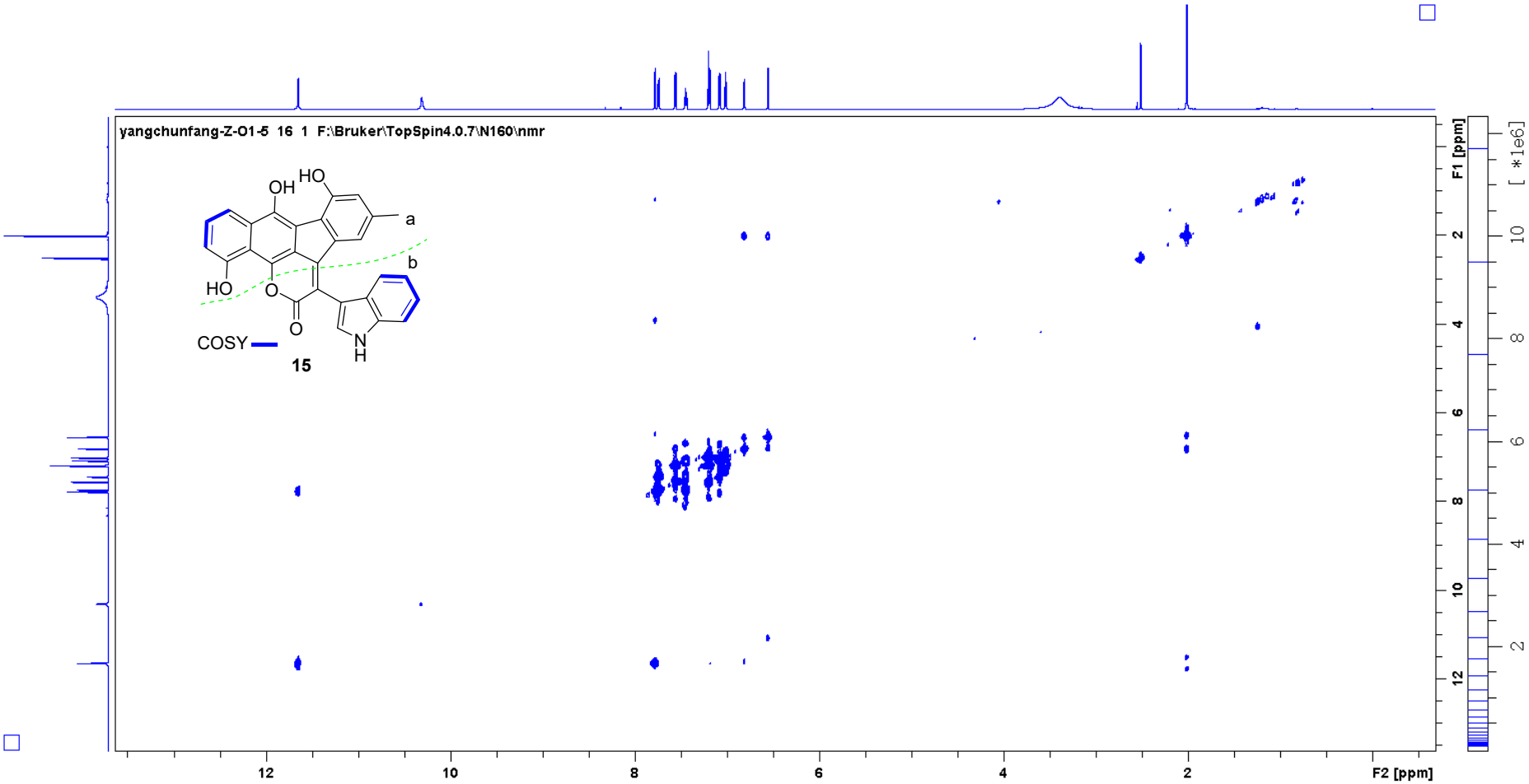

Figure S8. Spectroscopic data for fluostarene B (**15**). (continued).

(G) The HMBC spectrum of fluostarene B (**15**) in DMSO-d_6.

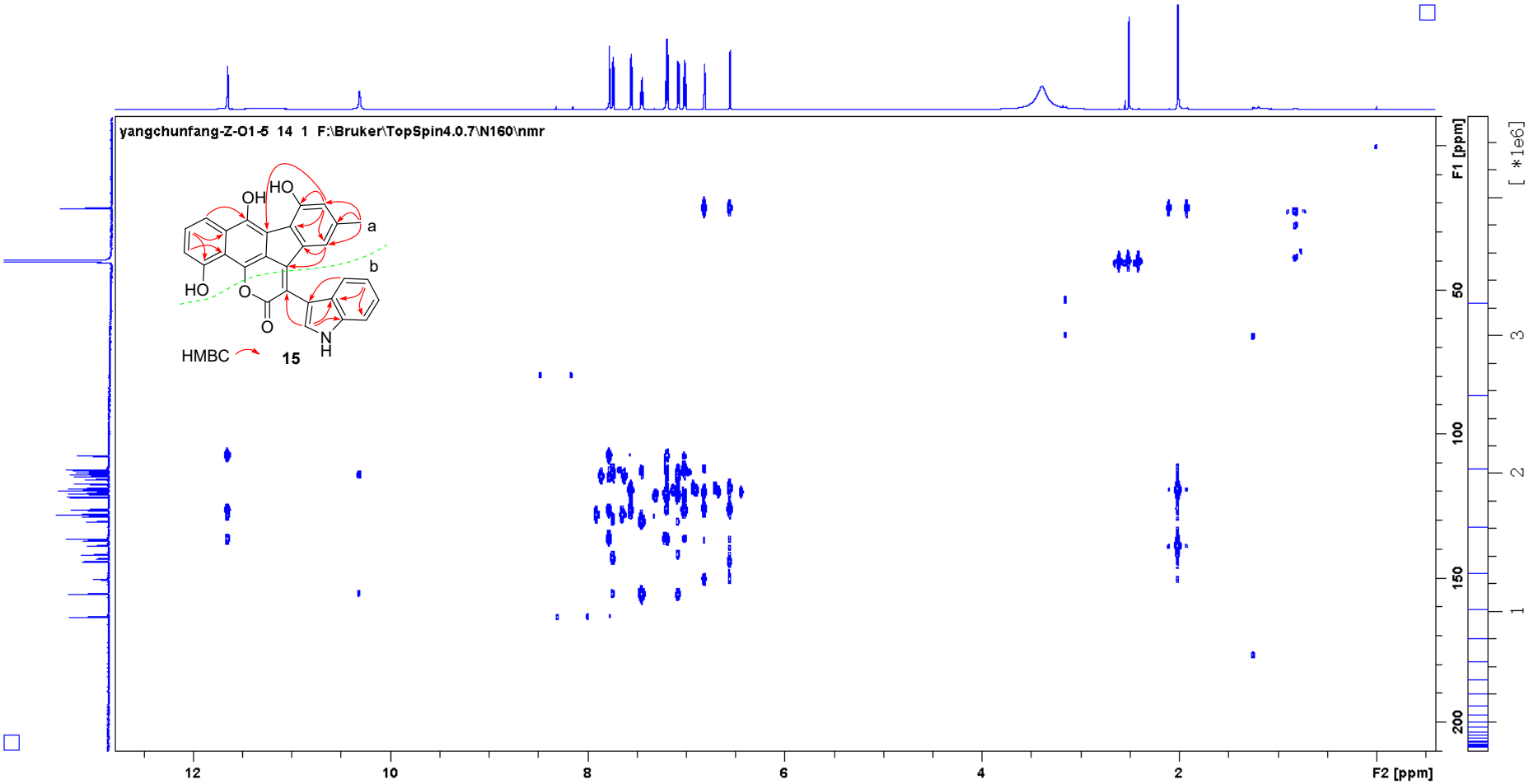

Figure S9. The HPLC profiles for *S. coelicolor* M1154-3 and *S. coelicolor* M1154-4 with *flsO1* and *alpK trans* complement to Δ*flsO1*i (*S. coelicolor* M1154-2) respectively.

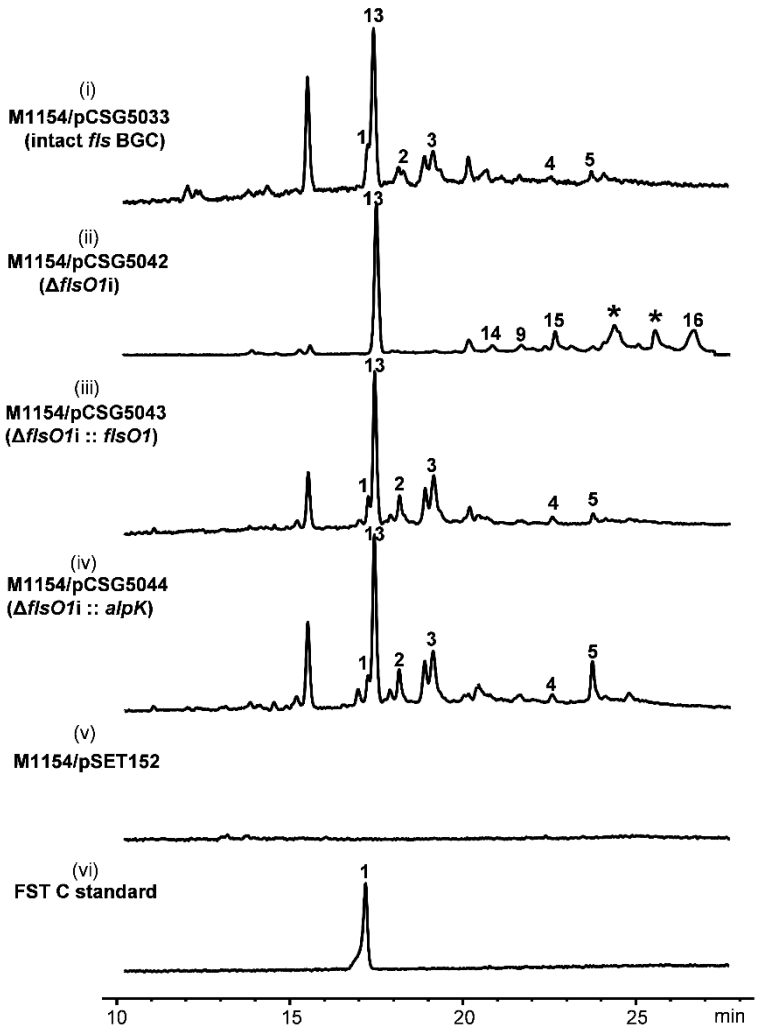

The fermentation profiles of Δ*flsO1*i (*S. coelicolor* M1154-2) and its complement strains (*S. coelicolor* M1154-3 and *S. coelicolor* M1154-4). (i) *S. coelicolor* M1154-1 (positive control), with pCSG5033 (containing intact *fls* BGC) expressed in *S. coelicolor* M1154; (ii) *S. coelicolor* M1154-2, with pCSG5042 (*flsO1* being in-frame deleted in pCSG5033) expressed in *S. coelicolor* M1154; (iii) complement Δ*flsO1*i (*S. coelicolor* M1154-2) with *flsO1*; (iv) complement Δ*flsO1*i (*S. coelicolor* M1154-2) with *alpK*; (v) negative control, with empty vector pSET152 expressed in *S. coelicolor* M1154; (vi) with fluostatin C as the authentic standard. The "*" in Figure S9 denotes uncharacterized benzofluorene-related products.

Figure S10. The proposed biosynthetic pathway of compounds **6** and **10**−**12**.

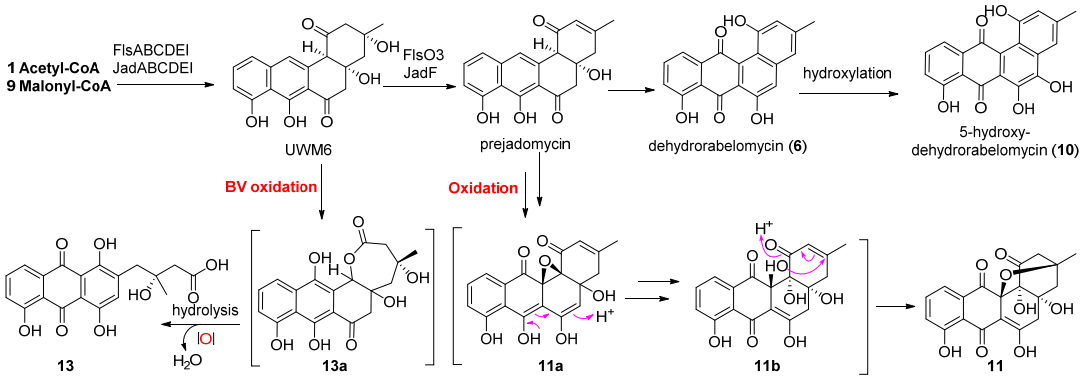

Supplementary References

(1) Datsenko, K. A.; Wanner, B. L. One-step inactivation of chromosomal genes in *Escherichia coli* K-12 using PCR products, *Proc. Natl. Acad. Sci. U S A* **2000**, *97*, 6640-6645.

(2) Paget, M. S.; Chamberlin, L.; Atrih, A.; Foster, S. J.; Buttner, M. J. Evidence that the extracytoplasmic function sigma factor sigmaE is required for normal cell wall structure in *Streptomyces coelicolor* A3(2), *J. Bacteriol.* **1999**, *181*, 204-211.

(3) Zhou, H.; Wang, Y.; Yu, Y.; Bai, T.; Chen, L.; Liu, P.; Guo, H.; Zhu, C.; Tao, M.; Deng, Z. A non-restricting and non-methylating *Escherichia coli* strain for DNA cloning and high-throughput conjugation to *Streptomyces coelicolor*, *Curr. Microbiol.* **2012**, *64*, 185-190.

(4) Zhang, W.; Liu, Z.; Li, S.; Lu, Y.; Chen, Y.; Zhang, H.; Zhang, G.; Zhu, Y.; Zhang, G.; Zhang, W.; Liu, J.; Zhang, C. Fluostatins I-K from the South China Sea-derived *micromonospora rosaria* SCSIO N160, *J. Nat. Prod* **2012**, *75*, 1937-1943.

(5) Wang, B.; Guo, F.; Ren, J.; Ai, G.; Aigle, B.; Fan, K.; Yang, K. Identification of Alp1U and Lom6 as epoxy hydrolases and implications for kinamycin and lomaiviticin biosynthesis, *Nat. Commun.* **2015**, *6*, 7674.

(6) Gust, B.; Challis, G. L.; Fowler, K.; Kieser, T.; Chater, K. F. PCR-targeted *Streptomyces* gene replacement identifies a protein domain needed for biosynthesis of the sesquiterpene soil odor geosmin, *Proc. Natl. Acad. Sci. U S A* **2003**, *100*, 1541-1546.

(7) Cherepanov, P. P.; Wackernagel, W. Gene disruption in *Escherichia coli*: TcR and KmR cassettes with the option of Flp-catalyzed excision of the antibiotic-resistance determinant, *Gene* **1995**, *158*, 9-14.

(8) Bierman, M.; Logan, R.; O'Brien, K.; Seno, E. T.; Rao, R. N.; Schoner, B. E. Plasmid cloning vectors for the conjugal transfer of DNA from *Escherichia coli* to *Streptomyces* spp, *Gene* **1992**, *116*, 43-49.

(9) Doumith, M.; Weingarten, P.; Wehmeier, U. F.; Salah-Bey, K.; Benhamou, B.; Capdevila, C.; Michel, J. M.; Piepersberg, W.; Raynal, M. C. Analysis of genes involved in 6-deoxyhexose biosynthesis and transfer in *Saccharopolyspora erythraea*, *Molecular & general genetics : MGG* **2000**, *264*, 477-485.

(10) Smokvina, T.; Mazodier, P.; Boccard, F.; Thompson, C. J.; Guérineau, M. Construction of a series of pSAM2-based integrative vectors for use in actinomycetes, *Gene* **1990**, *94*, 53-59.